



REGIONE  
TOSCANA



DIPARTIMENTO DI SCIENZE DELLA VITA  
DOTTORATO DI RICERCA IN SCIENZE DELLA VITA  
XXXIII CICLO

*Immunohistochemical studies of pulmonary remodeling in  
mice exposed to chronic cigarette smoke*

Settore Scientifico Disciplinare: MED-04

Relatore: Prof.ssa Monica Lucattelli  
*Dipartimento di Medicina molecolare e dello sviluppo*

Coordinatore: Prof. Massimo Valoti

Tesi di:

*Dott.ssa Emilia Balzano*

Anno Accademico 2020/2021

## INDEX

<i>Abstract</i>	<i>pag. 3</i>
<i>Introduction</i>	<i>pag. 5</i>
<i>Aim of the study</i>	<i>pag. 21</i>
<i>Materials and Methods</i>	<i>pag. 22</i>
<i>Results</i>	<i>pag. 27</i>
<i>Discussion</i>	<i>pag. 59</i>
<i>Conclusions</i>	<i>pag. 64</i>
<i>References</i>	<i>pag. 65</i>

## ABSTRACT:

Chronic Obstructive Pulmonary Disease (COPD) is a progressive and debilitating disease, associated primarily with cigarette smoke exposure, and it is characterized by chronic inflammation of the airways and lung parenchyma and changes in the pulmonary vasculature.

Four anatomic lesions are recognizable in COPD: emphysema, small airway remodeling (SAR), vascular remodeling, which may be associated with pulmonary hypertension, and chronic bronchitis, characterized by excessive mucus secretion. Several mechanisms are presumed to cause these changes and support related symptoms.

In particular, chronic inflammation and its related consequences, which include epithelial necrosis and apoptosis, changes in cell phenotype and function, proliferation and compartmentalization of specific cells in some pulmonary areas, and deposition of excessive extracellular matrix, have been implicated as the cause of the different clinical presentations of COPD.

Although a lot of studies have been carried out in the last twenty years, many facets of the pathogenesis of COPD are not fully understood.

Some murine strains mirror some human phenotypes after smoke exposure. Therefore, it was of interest to investigate in these strains whether changes in different endogenous factors, whose expression can influence alveolar destruction, repair and anatomical remodeling, are associated with changes characterizing different phenotypes of the disease. This study has been approached by using immunohistochemistry in order to have information on the expression and distribution of these factors in pulmonary structures at selected time points after the start of smoke exposure.

By using this methodological approach, the expression of important fibrogenic cytokines (i.e. TGF- $\beta$ , PDGF-B and CTGF) at various time points after cigarette smoke exposure have been investigated in C57 Bl/6J mice, which develop significant emphysema, and DBA/2 mice that develop changes similar to those of the "pulmonary fibrosis /emphysema syndrome". Some other factors that are indicative of apoptosis (cleaved caspase-3), senescence (p16<sup>ink4A</sup> and p21), regeneration (PCNA and Ki-67) or are implicated in fibrosis resolution and in apoptosis resistance (MyoD) were studied. In order to evaluate the involvement of these factors in parenchymal (i.e., vascular and peri-bronchiolar fibrosis) and airways remodeling (such as goblet cell metaplasia, fibrous and muscular remodeling), we used specific staining techniques (i.e., Masson's trichrome and PAS staining) or an immunohistochemical analysis for  $\alpha$ -SMA, at the various experimental time points.

A further investigation has been carried out to investigate the expression of three purinergic receptors (i.e. P2X<sub>4</sub>, P2X<sub>7</sub> and P2Y<sub>2</sub>), which have been recently involved in COPD pathogenesis by acting as danger signals and important mediators of inflammation.

The data obtained suggest that apoptosis, senescence and proliferation, that are induced at different rate and time points by inflammatory and fibrotic cytokines, play a role in early or late appearance of the remodeling processes that we observe in these strains of mice. Additionally, the necrosis of alveolar epithelial cells caused by enzyme release and oxidative damage (as revealed by MMP-9 and 8-OHdG positivity) characterize, at different extent, the lung responses of C57 Bl/6J and DBA/2 mice. The activation of purinergic receptors may be due to the release of alarmins, such as ATP and UTP, (which are the main ligands for P2X<sub>4</sub>, P2X<sub>7</sub> and P2Y<sub>2</sub>) following the necrosis of alveolar epithelial cells.

## INTRODUCTION:

Chronic Obstructive Pulmonary Disease (COPD) is a major cause of chronic morbidity and mortality throughout the world. It has been defined by GOLD as a disease state characterized by a progressive airflow limitation, measured during forced expiration, that is not fully reversible [Curtis JL *et al*, 2007]. The airflow limitation is usually associated with an abnormal inflammatory response of the lungs to noxious particles or gases [Pauwels RA *et al*, 2001].

The irreversible and progressive airflow limitation is caused by an increased resistance of small conducting airways, due mainly to the inflammatory and structural changes described in small airways, and by an increase in lung compliance due to emphysematous lung destruction [Hogg JC, 2004].

Risk factors for COPD include both host factors and environmental exposure. Although cigarette smoking has been firmly established as the most important risk factor for the development of COPD, other factors may be involved, including a genetic predisposition, which explains why only a small proportion of chronic heavy cigarette smokers develop COPD. Other risk factors include particulates or gases in environmental pollution and exposure to biomass combustion which could explain why some patients who develop COPD are never-smokers [Chung KF *et al*, 2008].

It is still difficult to give an exact definition of COPD because COPD is not *per se* a definite disease entity but rather a complex of conditions that contribute to airflow obstruction [Jeffery PK, 1999]. Four anatomic lesions are recognizable in COPD: emphysema, small airway remodeling (SAR), vascular remodeling, that may be associated with pulmonary hypertension, and excessive large airways mucus secretion (chronic

bronchitis) [Churg A *et al*, 2009]. Not all these lesions are always recognizable simultaneously in all COPD patients and they may be found differently associated in the individual patient.

Emphysema is probably the most studied anatomic lesion of COPD and is defined as an abnormal and permanent enlargement of airspace distal to terminal bronchioles accompanied by destruction of alveolar walls and without obvious fibrosis [Snider GL, 1989]. Over time several theories have been proposed to explain the pathobiology of emphysema: the protease-antiprotease hypothesis, the oxidant-antioxidant imbalance hypothesis or other theories that lay at the basis of the disease an inflammatory mechanism.

Oxidant-antioxidant imbalance is an important mechanism for the onset of COPD; CS and other harmful particles, upon inhalation, can produce excessive oxides, like superoxide anion ( $O^{2-}$ ) and nitric oxide (NO), which can directly damage lung tissue [Liang GB *et al*, 2019]. Oxides can not only directly destroy a lot of biochemical macromolecules such as proteins, lipids, and nucleic acids, thereby causing cell dysfunction and cell death, but can also destroy the extracellular matrix causing protease-antiprotease imbalance [Deslee G *et al*, 2009]. Destruction of elastic fibers is probably the central event in the pathogenesis of smoking-induced emphysema and several elastolytic enzymes in the lung have been suggested to be responsible for the onset of emphysema. In COPD patients, increased release of proteases such as matrix metalloproteinase and neutrophil elastase, which are capable of digesting structural proteins of the lung, may be found. Normally lung tissue is protected from proteolytic damage by a shield of protease inhibitors, principally derived from blood but also synthesized *in loco*, and emphysema occurs when protease-antiprotease imbalance favors proteolytic activity [Senior RM *et al*, 1998]. COPD is

characterized by chronic inflammation throughout the airways, lung parenchyma and pulmonary vasculature.

The number of inflammatory cells is increased approximately two to three times in lung of smokers. These cells may contribute to the local release of proteases and also to the production of reactive oxygen species (ROS) which are involved in alveolar destruction. Evidence supporting a role for these factors comes from human and animal studies and it is now accepted that they may all be differently involved.

Airway hypersecretion and ciliary dysfunction contribute to the morbidity of COPD leading to chronic bronchitis [Pauwels RA *et al*, 2001]. Epithelial goblet cells and mucus secreting glands are the major source of luminal mucus. Chronic irritation by cigarette smoke causes alteration in the biochemistry and in mucus rheology, as well as in the number and activity of secretory cells. Enlarged mucus-secreting glands (submucosal gland hypertrophy) and an increase in number of goblet cells (goblet cell hyperplasia) also in small bronchi or bronchioles are associated with mucus hypersecretion that contributes to the development of airflow obstruction in COPD. The end stage of COPD can also be characterized by epithelial atrophy, a decrease in the number of ciliated cells and ciliary abnormalities, such as giant cilia derived from the fusion of ciliary shafts, which may interfere with mucociliary clearance causing pooling of bronchial secretion [Jeffery PK, 1999 - Lungarella G *et al*, 1983 - Cosio MG *et al*, 1980].

Pulmonary arterial hypertension (PAH), which usually develops in the late course of COPD, is the main cardiovascular complication of the disease and it is associated with the development of *cor pulmonale* and a poor prognosis [McNee W, 1994 (1)]. PAH is characterized by a progressive increase in pulmonary vascular resistance leading to right ventricular failure and ultimately death. Remodeling of small pulmonary arteries represents

the main pathologic finding related to PAH, with endothelial dysfunction and marked proliferation of pulmonary artery smooth muscle cells, ending in the obstruction of resistance pulmonary arteries [Humbert M *et al*, 2004]. Medial hypertrophy in the muscular pulmonary arteries, and less commonly fibrinoid necrosis in these vessels, have been reported in patients with COPD who develop sustained pulmonary arterial hypertension. Small pulmonary arteries also develop accumulations of vascular smooth muscle cells in their intima and intimal thickening is an early event that occurs in association with progressive airflow limitation [McNee W, 1994 (2)]. Churg *et al* suggest that smoke exerts direct and rapid effects on vascular expression of vasoconstrictive, vasoproliferative and vasodilatory mediators with resulting endothelial dysfunction and vascular remodeling [Churg A *et al*, 2009].

A crucial pathologic feature of COPD is airway inflammation and remodeling at the level of small airways, defined as bronchioles that are less than 2 mm in diameter [Kim V *et al*, 2008]. Structural alteration and inflammation occurring at this level are considered to be the most important contributors to the airflow limitation in COPD patient accelerating the decline in FEV<sub>1</sub>(Forced expiratory volume in the 1st second). Small airway remodeling (SAR) is a variable combination of structural changes including epithelial denudation, myofibroblast proliferation, bronchiolar smooth muscle hypertrophy, mural edema, peribronchiolar and sub-epithelial fibrosis as well as the presence of inflammatory cells in the walls of membranous and respiratory bronchioles. Such changes may cause narrowing and distortion of airways lumina [Jeffery PK, 1999]. The pathogenesis of SAR is still being debated; two hypotheses have been formulated. One is that SAR represents a response to repeated inflammatory insults evoked by cigarette smoke so that the resulting changes in airway structure are a manifestation of aberrant healing processes induced by inflammatory cells. An alternative theory suggests that SAR is induced by an excessive production of



growth factors as a response to chronic injury and repair of the airway epithelium mediated by the inciting agent (*es.* cigarette smoke) which leads to increased muscle and fibrous tissue [Churg A *et al*, 2006].

Airway remodeling, though, does not affect only small airways but also central airways in COPD patients. An abnormal deposition of ECM proteins in sub-epithelial layers and an increase in smooth muscle mass has been demonstrated in the large airways of COPD patients when compared to control smokers. Sub-epithelial collagen deposition inversely correlates with the FEV<sub>1</sub>/ FVC ratio and FEV<sub>1</sub> suggesting that an abnormal protein deposition at this level could also play a role in the development of airflow obstruction [Pini L *et al*, 2014].

One of the critical steps in the remodeling process is the proliferation of fibroblasts and myofibroblasts and the thickening of bronchial walls, which is mainly related to an increase in connective tissue deposition induced by fibroblasts activation. Some growth factors are able to modulate the proliferation of fibroblasts and the synthesis of extracellular matrix components [Kovacs EJ *et al*, 1994] and their involvement in COPD pathogenesis has been studied. Growth factors like transforming growth factor  $\beta$  (TGF- $\beta$ ) has been demonstrated to be up-regulated in chronic bronchitis and the increased expression of TGF- $\beta$  is usually significantly correlated with the thickness of the basal membrane and the number of fibroblasts [Vignola AM *et al*, 1997]. TGF- $\beta$  enhances airway smooth muscle proliferation and ECM deposition by activated fibroblasts and modulates airway smooth muscle shortening and hyperresponsiveness [Saito A *et al*, 2018].

TGF- $\beta$  signaling, through a Smad dependent pathway, drives the production of other genes like Connective Tissue Growth Factor (CTGF) which is believed to be the proximate

mediator of collagen induction in fibroblasts. CTGF gene expression has been demonstrated to be up-regulated after chronic exposure to cigarette smoke [Churg A *et al*, 2006]. Moreover, since the combined action of TGF- $\beta$  and CTGF induces TIMPs, thereby preventing matrix degradation [Bonniaud P *et al*, 2004], it has been suggested that CTGF is necessary for the progression and persistence of a fibrogenic [Lasky JA *et al*, 1998] response.

Myofibroblasts are multifunctional cells and they play critical roles in wound healing and in fibrosis [Wynn T, 2008]; they regulate connective tissue remodeling by combining the extracellular matrix (ECM)-synthesizing features of fibroblasts with cytoskeletal characteristics of contractile smooth muscle cells. Myofibroblasts are present in few normal tissues with high remodeling capacity like lungs [Phan SH, 2002]. In injured tissue, quiescent fibroblasts can differentiate into myofibroblasts [Li B *et al*, 2011]. Smooth muscle cells (SMC) and fibrocytes from blood are also potential source of myofibroblasts. The differentiation of myofibroblasts from fibroblasts and SMC is a common response in wound healing. This process is triggered by many cytokines and growth factors including TGF- $\beta$  and CTGF. Additionally, TGF- $\beta$  induces myogenic differentiation factor D (MyoD) which is a master regulator of the terminal differentiation of skeletal muscle and is capable of inducing fibroblasts to differentiate into myofibroblasts and muscle cells to de-differentiate into myofibroblasts [Hecker L *et al*, 2011 - Serrano AL *et al*, 2010]. Once the repairing process is over, myofibroblasts are thought to undergo apoptosis, but their inability to terminate the reparative process associated with persistent activation and accumulation of these cells in tissue can lead to resemble fibrosis. It has also been suggested that epithelial and endothelial cells may change their phenotype to mesenchymal cells, in response to TGF- $\beta$  signaling [Saitoh M, 2015], through processes described as epithelial-mesenchymal transition (EMT) and endothelial to mesenchymal transition

(EndMT) respectively. Such mechanisms may also be source of myofibroblasts in pulmonary fibrosis [Willis BC *et al*, 2006].

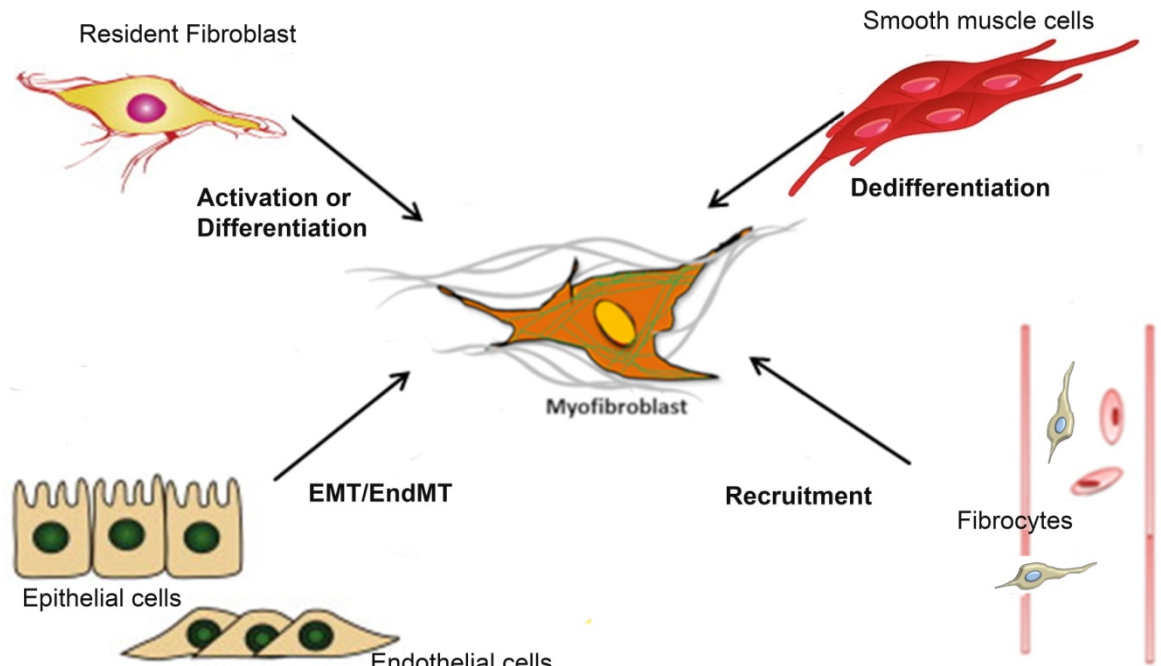


Figure 1. Multiple origins of myofibroblasts.

Activated myofibroblasts express  $\alpha$ -smooth muscle actin ( $\alpha$ -SMA) and show an increased proliferation, migratory ability and production of cytokines and interstitial matrix [Hinz B *et al*, 2012].

Cellular senescence is defined as an irreversible cell cycle arrest so that the proliferation is blocked even in presence of mitogen factors. Several markers are associated with cellular senescence among which p16<sup>ink4A</sup> and p21CIP1/WAF1, cyclin-dependent kinase inhibitors that act as sensors of cellular stress and are involved in cell-cycle growth arrest and eventually apoptosis. Chronic smoke exposure has been reported to increase the expression of p21 in alveolar epithelial cells type II and bronchial cells [Chiappara G *et al*, 2014]. Senescence and apoptotic resistance are other mechanisms that have been postulated to be involved in the fibrogenic process; recent studies have demonstrated that senescent myofibroblasts accumulate in the lung of IPF patients. They persistently express MyoD

and are resistant to apoptosis and dedifferentiation thus contributing to established fibrosis [Kato K *et al*, 2020].

Platelet derived growth factor (PDGF) is considered a potent mitogen and chemo-attractant for myofibroblasts that drives the recruitment and replication of these cells at sites of tissue injury. In human disease and in animal models of pulmonary fibrosis, PDGF expression correlates with the expansion of the myofibroblasts population that ultimately contributes to the production of extracellular matrix proteins such as collagen, fibronectin, and glycosaminoglycans [Bonner JC, 2004]. PDGF can be produced by airway and alveolar epithelial cells in fibrotic condition [Antoniades HN *et al*, 1990] and may play a role in airway remodeling in asthma [Ingram JL *et al*, 2004]. Interestingly, the inhibition of PDGF signaling can prevent fibrosis in some murine model [Abdollahi A *et al*, 2005]. Expression of PDGF and PDGF receptors is also increased in the lung arteries of patients with pulmonary arterial hypertension and induces proliferation and migration of smooth muscle cells in human pulmonary artery [Perros F *et al*, 2008].

It is increasingly clear that subtle fibrotic reactions are associated with airway and vascular remodeling in diseases such as asthma, chronic bronchitis and chronic obstructive pulmonary disease and that all the mechanisms mentioned above may contribute to the remodeling typical of COPD patients.

As previously said, COPD is characterized by chronic inflammation throughout the airways, parenchyma and pulmonary vasculature. Chronic inflammation is characterized by accumulation of neutrophils, macrophages, B-cells and CD8<sup>+</sup> T-cells. Each of these inflammatory cell types is involved in the pathogenesis of COPD through the stimulation of the synthesis of inflammatory mediators such as cytokines, chemokines, growth factors, nitric oxide and reactive oxygen species (ROS). ROS can directly damage lung cells or can

promote the release of damage associated molecular patterns (DAMPs), which can further trigger the inflammatory response. Recently numerous studies have generated data supporting the hypothesis that extracellular adenosine 5-triphosphate (ATP) is involved in the pathogenesis of COPD acting as an important danger signal and an important mediator of inflammation [Mortaz E *et al*, 2009]. The extracellular concentration of ATP, that is usually low and tightly regulated by ectonucleotidases, can markedly rise during hypoxia, infection or inflammation, either by active or passive release from various cell types and/or by down-regulation of ectonucleotidases [Aliagas E *et al*, 2018].

Increased extracellular ATP level has been found in BALF from COPD patients and its signaling has been suggested to be involved in smoke induced lung injury and emphysema [Lommatzsch M *et al*, 2010].

Purines and pyrimidines actions are mediated by purinergic receptors which are distinguished in two types and are identified as P1, which binds adenosine, and P2, which binds mostly ATP.

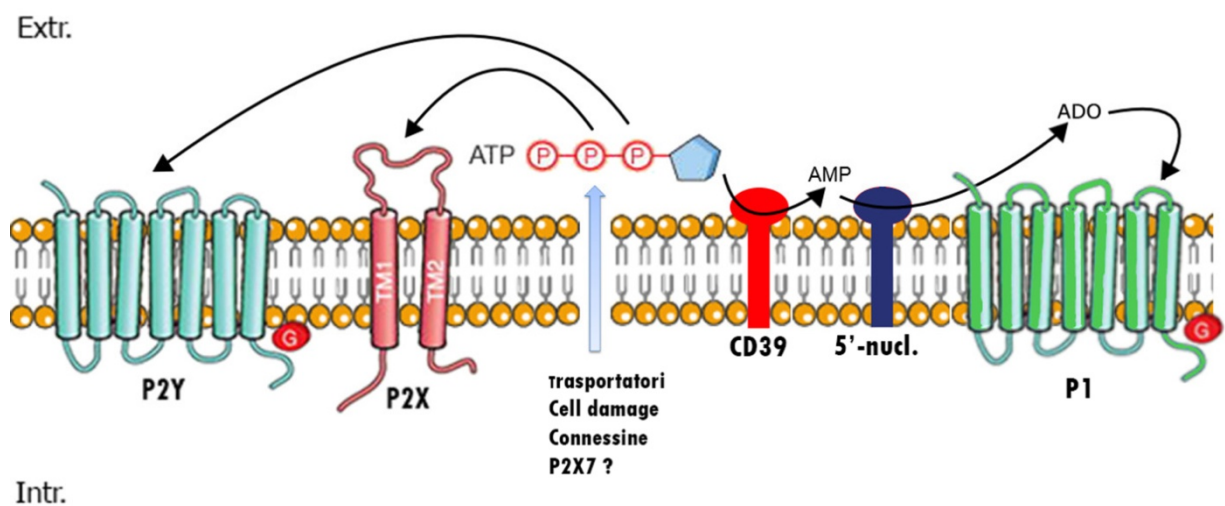


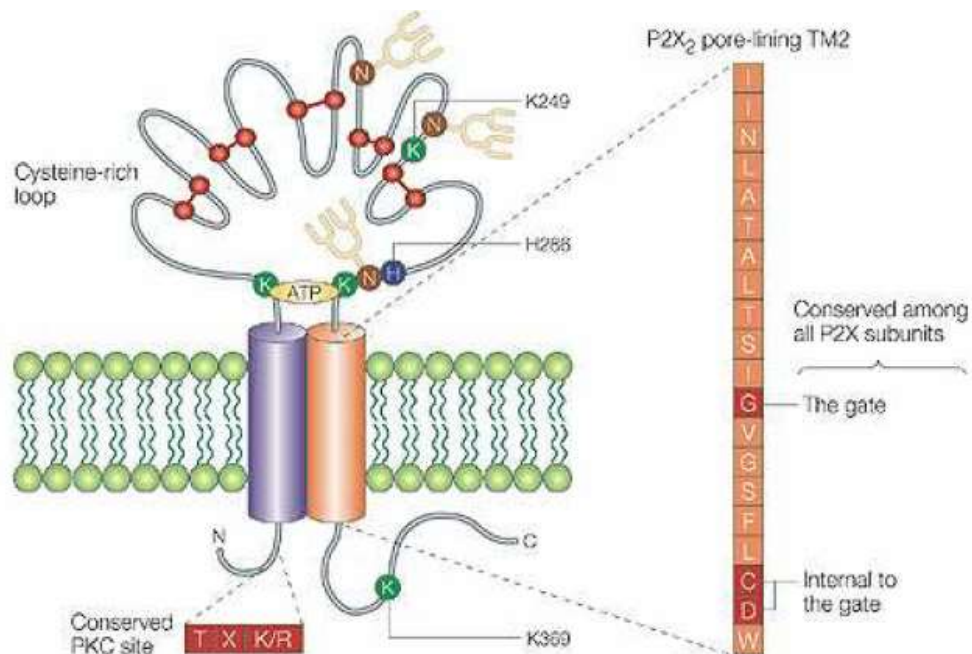
Figure 2. Components of purinergic signaling system.

P1 receptors are G protein-coupled membrane receptors which bind adenosine and comprises A<sub>1</sub>, A<sub>2A</sub>, A<sub>2B</sub> and A<sub>3</sub> receptors.

P2 receptors instead bind mainly ATP and can be divided in 2 sub-families:

- P2Y receptors, which are 7 domain trans-membrane metabotropic receptors and
- P2X receptors, which are ionotropic receptors [Abbracchio MP *et al*, 1998]

**P2X** receptors are a family of ligand-gated, non-selective cation channels that open in response to the binding of extracellular ATP. P2X receptor subunits are encoded by seven genes and are 36–48% identical to one another at the amino acid level. Each subunit has two hydrophobic transmembrane domains separated by an extracellular domain, a short NH<sub>2</sub> terminus (20-30 aa) and longer COOH tail which are cytoplasmatic [Newbolt A *et al*, 1998]. The extracellular domains contain 10 cysteine residues that bind to form disulfide bonds, which allow the preservation of the structure needed to link the binding site for ATP and the ion channel [Ralevic V *et al*, 1998]. All P2X receptor subunits have three to six consensus sequences for N-linked Glycosilation in the extracellular loop and the deletion of two of them greatly impairs the functional expression of the receptor [Torres GE *et al*, 1998]. COOH terminus modifications, instead, alter the kinetics, the desensitization and the permeability of the channel in different ways [Smith FM *et al*, 1999]. P2X subunits are 379 (P2X<sub>6</sub>) to 595 (P2X<sub>7</sub>) amino acids long and include a binding site for protein kinase C in the short NH<sub>2</sub> terminus [Boue-Grabot E *et al*, 2000] and an ATP binding site in the extracellular loop, probably near the channel vestibule [Ennion S *et al*, 2000].



© Sara Gulinelli, Caratterizzazione degli effetti mediati dalla stimolazione dei recettori P2 in cheratinociti e macrofagi umani.

Figure 3. Schematic representation of P2X receptor.

The functional P2X receptor is a multimeric unit, which can form as homomers or heteromers and at least two different subunits can contribute to the ion channel.

<i>P2X subtype</i>	<i>Length aa</i>	<i>Main agonist</i>
P2X <sub>1</sub>	399	ATP
P2X <sub>2</sub>	471	ATP
P2X <sub>3</sub>	397	ATP
P2X <sub>4</sub>	388	ATP
P2X <sub>5</sub>	422	ATP
P2X <sub>6</sub>	441	ATP
P2X <sub>7</sub>	595	ATP

Tab 1. P2X subunits

Seven homomeric receptors, named from one to seven, and four heterotrimeric (P2X<sub>2/3</sub>, P2X<sub>1/5</sub>, P2X<sub>2/6</sub> and P2X<sub>4/6</sub>) receptors have been identified and characterized. All P2X receptors are permeable to small monovalent cations but some have a significant calcium or anion permeability as well. The opening of P2X channels induces an influx of ions like

$\text{Na}^+$  and  $\text{Ca}^{2+}$  and a  $\text{K}^+$  efflux through the membrane, which lead to plasma membrane depolarization and the activation of  $\text{Ca}^{2+}$  signaling cascade such as p38 MAPK or phospholipase  $\text{A}_2$  activation following the increase of intracellular  $\text{Ca}^{2+}$  levels [Idzko M *et al*, 2014].  $\text{P2X}_2$ ,  $\text{P2X}_4$  and  $\text{P2X}_7$  seem to have at least two pore dilatations ( $\text{I}_1$  and  $\text{I}_2$ ) and different permeability following ATP concentration. Low concentration of ATP or a brief stimulation lead to a small ion channel (0,9 nm in  $\text{P2X}_7$ ), which is not permeable to organic or large cations ( $\text{I}_1$ ). The opening happens within few milliseconds. Sustained activation of these channel, instead, consents the development of a larger pore (3-5 nm), which allows the flow of large cations for about a hundred milliseconds ( $\text{I}_2$ ) [Virginio C *et al*, 1999 (1)-Virginio C *et al*, 1999 (2)].  $\text{P2X}$  receptors play key roles in various physiological process such as nerve transmission, pain sensation and immune response [North RA, 2002].

$\text{P2X}_4$  preferentially assembles as homotrimers and is exclusively activated by ATP. High level of expression has been found in bronchial epithelial cells, alveolar epithelial type I cells, lamellar bodies of alveolar type II cells, alveolar macrophages and smooth muscle cells [Burnstock G *et al*, 2012].  $\text{P2X}_4$  is also the most abundantly expressed  $\text{P2X}$  receptor in vascular endothelial cells. Several studies demonstrated the involvement of this receptor in allergen induced airway inflammation [Zech A *et al*, 2016]. A strict relation has also been found between  $\text{P2X}_4$  and inflammation-induced mucous metaplasia and hyperplasia [Winkelmann VE *et al*, 2019], alterations of endothelial cell response to flow stimulation, and with hypoxia, leading to structural remodeling of vessels [Yamamoto K *et al*, 2006]. Chen *et al*. also demonstrated that the signaling originated from the binding of ATP to  $\text{P2X}_4\text{R}$  may contribute to airway remodeling in allergic asthma in mice and it could be required for collagen deposition [Chen H *et al*, 2016]. Furthermore, Wang L. and colleagues suggested that  $\text{P2X}_4$  contributes to airway remodeling in a mouse model of



allergic asthma by favoring the proliferation of bronchial smooth muscle cells induced by PDGF-B through the expression of p38MAPK [Wang L *et al*, 2018].

*P2X<sub>7</sub>* is the last cloned P2X receptor and it is activated by ATP, especially in its tetra-anionic form (ATP<sup>4-</sup>), while ADP and AMP are very weak agonists. It assembles only as a homotrimer and it shows no desensitization; prolonged ATP exposure or higher concentrations of ATP lead to the transition from an ion channel to an unselective pore that allows the transit of bigger molecules [North RA, 2002]. *P2X<sub>7</sub>* differs from other P2X receptors because of a long COOH terminus which seems to be necessary for the formation of the pore. The formation of the pore is not reversible unless the ligand is removed so this phenomenon is usually associated with cito-toxicity. [Surprenant A *et al*, 1996]. After 30 seconds of application of 2'(3')-O-(Benzoyl-4-benzoyl)-ATP or ATP the plasma membrane begins to develop large blebs, which become multiple and sometimes coalesce in a few minutes. Membrane blebs then develop as large and hemispherical protrusions of plasma membrane [North RA, 2002].

*P2X<sub>7</sub>* is expressed in airway epithelium and in fibroblasts and there is increasing evidence to support that the *P2X<sub>7</sub>* receptor is involved in signaling between macrophages or other cells involved in the immune response and target cells. Chronic smoke induces inflammation, which is associated with increased levels of this receptor on blood and airway neutrophils, alveolar macrophages and in whole lung tissue. *P2X<sub>7</sub>* is implicated in the release of reactive oxygen species (ROS), cytokines like IL-6 and IL-1 $\beta$  and matrix metalloprotease-9 (MMP-9) by immune cells and recent studies suggest the involvement of this receptor in the pathogenesis of the emphysema associated with COPD [Lucattelli M *et al*, 2011 - Eltom S *et al*, 2011]. IL-6 and IL-1 $\beta$  have been shown upregulate the expression

of fibrotic factors like TGF- $\beta$  *via* an NF- $\kappa$ B/AP1 pathway, thus contributing to the fibrotic process [Robert S *et al*, 2016- Saito F *et al*, 2008].

Riteau and colleagues demonstrated that ATP and P2X<sub>7</sub>R are involved in inflammation and remodeling process in a mouse model of bleomycin induced pulmonary fibrosis [Riteau N *et al*, 2010].

A compensatory mechanism for the expression of P2X<sub>7</sub> and P2X<sub>4</sub> has been documented in mouse lung epithelial cells and in rodent immune cells: the down-regulation of one stimulate the up-regulation of the other [Weinhold K *et al*, 2010].

**P2Y** receptors show the characteristic seven hydrophobic transmembrane domains. They are 328-377 aa long with a short extracellular NH<sub>2</sub> terminal and an intracellular COOH terminal for a total weight, after glycosilation (N11,27,223,197), of 41-53 kDa [Abbracchio MP *et al*, 1998]. The amino acid sequence of these receptor is highly heterogeneous. The structural diversity of the intracellular loops and the COOH-terminal among the different P2Y subtypes determine the coupling with different G proteins [Fischer W *et al*, 2007].

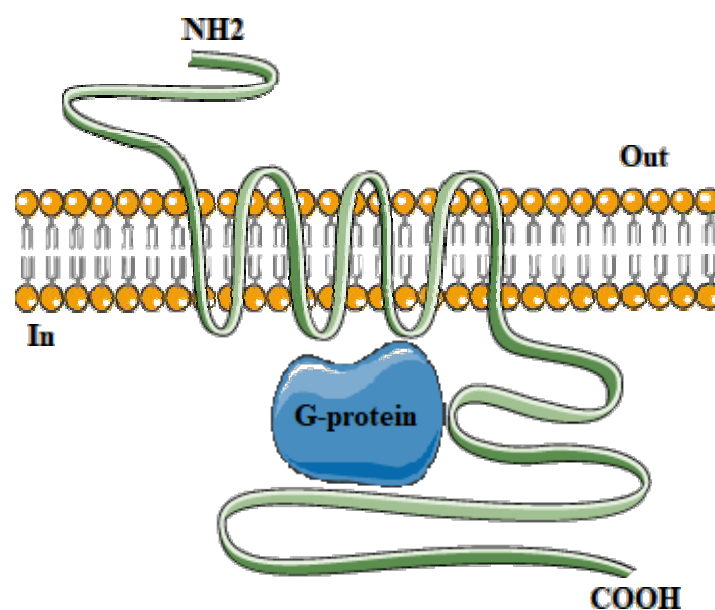


Figure 4. Schematic representation of P2Y receptor.

Moreover, the C-terminus has consensus binding motifs for protein kinases A and C. These receptors are activated by low concentration of ATP and the duration of the signal may last from a hundred of milliseconds to a few seconds even if they are sensitive to different nucleotide. ADP is the main agonist of P2Y<sub>1</sub>, P2Y<sub>12</sub> and P2Y<sub>13</sub>; ATP and UTP are equivalent in activating P2Y<sub>2</sub>, while UTP and UDP are the main agonists of P2Y<sub>4</sub> and P2Y<sub>6</sub>; P2Y<sub>11</sub> is activated only by ATP but it is not expressed in mice. P2Y<sub>14</sub> is different from other receptors: it is activated by UDP-glucose [Chambers JK *et al*, 2000].

Some positively charged amino acid residues in transmembrane regions 3, 6, and 7 may be involved in the binding to phosphates of ATP. Neutralization of positive amino acids in transmembrane regions 6 and 7 causes a 100- to 850-fold decrease in the potency of ATP and UTP [Erb L *et al*, 1995].

<i>P2Y subtype</i>	<i>Length in aa</i>	<i>Main agonist</i>
<b>P2Y<sub>1</sub></b>	373	ADP
<b>P2Y<sub>2</sub></b>	377	UTP, ATP
<b>P2Y<sub>4</sub></b>	365	UTP
<b>P2Y<sub>6</sub></b>	328	UDP
<b>P2Y<sub>11</sub></b>	374	ATP
<b>P2Y<sub>12</sub></b>	342	ADP
<b>P2Y<sub>13</sub></b>	354	ADP
<b>P2Y<sub>14</sub></b>	338	UDP-glucose

*Tab.2 P2Y receptors*

The P2Y receptor family is further divided in 2 subfamilies: the P2Y<sub>1</sub> subfamily, which includes receptors coupled with a G<sub>q</sub> protein (P2Y<sub>1</sub>, P2Y<sub>2</sub>, P2Y<sub>4</sub>, P2Y<sub>6</sub> and P2Y<sub>11</sub>) therefore activating phospholipase C and the P2Y<sub>12</sub> subfamily, which includes receptors

coupled with  $G_i$  protein (P2Y<sub>12</sub>, P2Y<sub>13</sub> and P2Y<sub>14</sub>) [Harden TK *et al*, 2010]. The binding between ATP and a P2Y receptor coupled with  $G_q$  protein leads to calcium release from intracellular storage *via* phospholipase C/IP<sub>3</sub> activation, while the binding with a  $G_i$ -coupled receptor inhibits adenylate cyclase [Idzko M *et al*, 2014]. Interaction between P2Y receptors has been demonstrated and formation of oligomers greatly increases the diversity of purinergic signaling. Interaction between a P2Y receptor and other G protein-coupled receptors, for example adenosine A1 receptor, has been demonstrated [Burnstock G, 2007]. P2Y receptors are widely expressed in brain, airways epithelia, gastrointestinal tract, eye, vascular system and immune and inflammatory cells [Harden TK *et al*, 2010]. The activation of several mitogen-activated protein kinases (MAPKs), in particular extracellular signal-regulated protein kinase 1/2 (ERK 1/2), is commonly associated with the stimulation of several P2Y receptors [Burnstock G, 2007].

P2Y<sub>2</sub> is a  $G_q$  protein coupled receptor, and both ATP and UTP have the same potency as agonists. P2Y<sub>2</sub> receptor is widely and highly expressed in lung, heart, skeletal muscle, myofibroblasts and immune cells such as lymphocytes and macrophages; it is also expressed in smooth muscle cells and in endothelial cells of vessels, where it induces vasodilatation [Ralevic V *et al*, 1998]. Activation of the P2Y<sub>2</sub> receptor promotes proliferation of many cell types, including airway epithelial cells, and it is crucial for some leukocyte function such as neutrophils chemotaxis and the production of mediators by neutrophils, eosinophils and macrophages. Interestingly, several studies suggest an ambivalent function for P2Y<sub>2</sub>; it can act as a "friend" in case of a bacterial infection but, in case of chronic lung disease, inappropriate activation can lead to uncontrolled inflammation and fibrotic remodeling [Idzko M *et al*, 2014]. ATP, through the activation of P2Y<sub>2</sub>, acts as an autocrine and paracrine mediator of vascular remodeling and adventitial thickening, thus stimulating endothelial and fibroblast proliferation. MMP-9 is an

extracellular zinc endopeptidase with the ability to cleave extracellular matrix components. It can also be involved together with his inhibitor TIMP-1, in the pathogenesis of lung fibrosis [Riteau N *et al*, 2010]. It has been demonstrated that MMP-9 may be induced by P2Y<sub>2</sub> signaling [van der Vliet A *et al*, 2011]. P2Y<sub>2</sub>R is also upregulated in mice model of pulmonary fibrosis and studies carried out on fibroblasts derived from wild type and P2Y<sub>2</sub><sup>-/-</sup> mice showed an increased migration and proliferation. This suggests a role of this receptor in tissue remodeling and fibrosis.

Other studies suggest that P2Y<sub>2</sub> signaling may induce IL-6 secretion [Müller T *et al*, 2017], as well as tissue destruction and lung inflammation following cigarette smoke exposure [Cicko S *et al*, 2010].

#### AIM OF THE STUDY:

The aim of this study was to investigate the mechanism underlying the pulmonary remodeling associated with COPD in mice chronically exposed to cigarette smoke. In particular, we sought to understand the role of proliferation, senescence and apoptosis of the various cell types involved in the disease, and the role of profibrotic cytokines in the induction of the process.

Moreover, since the involvement of purinergic receptor(s) in the pathogenesis of some anatomic changes in COPD, like inflammation and emphysema, has been previously proved, we tried to determine if these receptors may play a role also in the remodeling processes.

## MATERIALS AND METHODS:

*Animals:* C57 BL/6J and DBA/2 male two months old mice (purchased from Charles River Italia, Calco, Italy) were used in this study. The mice were housed at room temperature (22 to 24°C) with relative humidity of 40-50%. Food and water were supplied *ad libitum*.

*Chronic exposure to cigarette smoke:* C57 BL/6J and DBA/2 mice were exposed to the smoke from three cigarettes (CS) (Marlboro Red, 10 mg of tar and 0.8 mg of nicotine) per day, 5 days/week for 1, 4, 7 and 11 months in specifically designed cages according to Cavarra and colleagues. The smoke is produced by the burning of a cigarette and introduced into the chamber with the airflow generated by a mechanical ventilator at the rate of 33 ml/min; a second ventilator is used to provide room air for dilution 1:8 of the smoke stream [Cavarra E *et al*, 2001]. Control mice were exposed to room air under the same conditions. At the different time points animals were anesthetized and sacrificed by severing the abdominal aorta.

*Morphology and morphometry:* Mice lungs were fixed intra-tracheally with buffered formalin (5%) at a constant pressure of 20 cm H<sub>2</sub>O for 5 hours then dehydrated, cleared in toluene and embedded in paraffin. Multiple 6 µm latero-sagittal lung section were made.

Two lung sections were stained with Masson's trichrome staining in order to evaluate the entity of collagen deposition. Goblet cell metaplasia was evaluated by Periodic acid–Schiff (PAS) reaction. Because usually there aren't any goblet cells in murine bronchi, a mouse is considered to have developed goblet cell metaplasia when at least one or more middle size bronchi show positive PAS staining. The percentage of animals developing goblet cell metaplasia is calculated evaluating pulmonary sections from 8 mice.

The morphometrical evaluation of emphysema was performed on hematoxylin-eosin stained sections using the determination of the "mean linear intercepts" (Lm) and of the internal surface area (ISA) calculated according to the formula  $ISA=4xVL/Lm$  where VL is the post fixation lung volume [Thurlbeck WM, 1967 (1)]. For the determination of Lm two blinded pathologists evaluated 40 histologic fields for each pair of lungs, both vertically and horizontally [Thurlbeck WM, 1967 (2)].

*Immunohistochemical analysis:* 5  $\mu$ m tissue sections from mice exposed to room air or CS for 1, 4, 7 and 11 months were stained for  $\alpha$ -smooth muscle actin ( $\alpha$ -SMA), transforming growth factor- $\beta$  (TGF-  $\beta$ ), connective tissue growth factor (CTGF), platelet derived growth factor-B (PDGF-B), 8-oxo-7,8-dihydro-2'-deoxyguanosine (8-OHdG), cleaved caspase-3, p16<sup>ink4A</sup>, p21, proliferating cell nuclear agent (PCNA), Ki-67, MyoD, P2Y<sub>2</sub>, P2X<sub>4</sub>, P2X<sub>7</sub>, interleukin-6 (IL-6) and Matrix Metalloproteinase 9 (MMP-9).

Antigen retrieval was performed by heating the sections in a microwave (750W) in 0.01 M pH 6.0 citrate buffer for:

- 20 min for the immunodetection of 8-OHdG, p16<sup>ink4A</sup>, PCNA, Ki-67, caspase-3 and MyoD,
- 16 min for the immunodetection of PDGF-B,
- 15 minutes for the immunodetection of p21,
- 12 minutes for TGF- $\beta$ ,
- 10 minutes for the immunodetection of P2X<sub>7</sub> and P2Y<sub>2</sub>,
- 8 minutes for the immunodetection of MMP-9 and
- 5 minutes for P2X<sub>4</sub>

For the immunodetection of IL-6 antigen retrieval was performed by heating the sections for 10 minutes in a microwave at 600W in 0.01 M pH 6.0 citrate. All the sections were

allowed to cool slowly to room temperature (RT). No antigen retrieval was used for the immunodetection of  $\alpha$ -SMA and CTGF. All the sections, except the ones used for the immunodetection of P2Y<sub>2</sub> and Caspase-3, were pre-treated with 3% hydrogen peroxide for blocking the endogenous peroxidase and then incubated with 3% bovine serum albumin for 30 minutes at room temperature to block non-specific antibody binding.

Sections were incubated overnight at 4°C with the primary antibodies: rabbit polyclonal Ab to TGF- $\beta$  (Novus Biological, Centennial, CO, USA) diluted 1:50, rabbit polyclonal Ab to CTGF (Abcam, Cambridge, UK) diluted 1:200, rabbit polyclonal Ab to PDGF-B (Abcam, Cambridge, UK) diluted 1:100, rabbit polyclonal Ab to Caspase-3 (Cell signaling technology, Danvers, MA, USA) diluted 1:300, rabbit polyclonal Ab to Ki-67 (Abcam, Cambridge, UK) diluted 1:100, rabbit polyclonal Ab to P2Y<sub>2</sub> (Novus Biological, Centennial, CO, USA) diluted 1:150, rabbit polyclonal Ab to P2X<sub>4</sub> (Biorbyt, Cambridge, UK) diluted 1:100, rabbit polyclonal Ab to P2X<sub>7</sub> (Novus Biological, Centennial, CO, USA) diluted 1:350 and rabbit polyclonal Ab to MMP-9 (Novus Biological, Centennial, CO, USA) diluted 1:400.

After rinsing with PBS, TGF- $\beta$ , Ki-67, P2X<sub>4</sub> and P2X<sub>7</sub> slides were incubated with sheep anti-rabbit IgG diluted 1:200 (Sigma, St. Louis, MO, USA) and PDGF-B slides with the same antibody diluted 1:100 for 30 minutes at RT followed by incubation with peroxidase-antiperoxidase complex (Sigma, St. Louis, MO, USA) prepared from rabbit serum.

CTGF and MMP-9 sections were incubated with the appropriate biotin-conjugated secondary antibody (Vector Labs, Burlingame, CA) diluted 1:200 and subsequently with streptavidin-HRP complex (BD bioscience, San Diego, CA, USA) diluted 1:1000 with PBS+BSA.



Color development was performed using 3,3'-diaminobenzidine tetra hydrochloride as a chromogen (DAB; Vector Laboratories, Burlingame, CA).

The sections for P2Y<sub>2</sub> and cleaved caspase-3 were rinsed in PBS and incubated with goat polyclonal anti-rabbit biotinylated IgG (1:200) (Vector Labs, Burlingame, CA) for 30 minutes at room temperature. The staining was revealed by adding Streptavidin-alkaline phosphatase (BD Pharmingen, Buccinasco, Italy).

Color development was performed using nitro-blue tetrazolium chloride (NBT) and 5-bromo-4-chloro-3'-indolyphosphate p-toluidine salt (BCIP).

$\alpha$ -SMA protein, 8-OHdG, p16<sup>ink4A</sup>, p21, PCNA, IL-6, and MyoD were immunohistochemically evaluated using the Vector<sup>®</sup> M.O.M<sup>™</sup> immunodetection kit (Vector Laboratories, Burlingame, CA), designed specifically to localize mouse primary monoclonal and polyclonal antibodies on mouse tissues by using a novel blocking agent and reducing undesired background staining, and DAB (Vector Laboratories, Burlingame, CA) as substrate. Paraffin sections were incubated using mouse monoclonal Ab to  $\alpha$ -SMA (Sigma, St. Louis, MO, USA) diluted 1:300, mouse monoclonal Ab to 8-OHdG (Abcam, Cambridge, UK) diluted 1:500, mouse monoclonal Ab to p16<sup>ink4A</sup> (Abcam, Cambridge, UK) diluted 1:200, mouse monoclonal Ab to p21 (Novus Biological, Centennial, CO, USA) diluted 1:300, mouse monoclonal Ab to PCNA (Dakocytomation, Glostrup, Denmark) diluted 1:100, Mouse monoclonal Ab to MyoD (Novus Biological, Centennial, CO, USA) diluted 1:50 and mouse monoclonal Ab to IL-6 (Proteintech group, Rosemont, IL, USA) diluted 1:300. Slides immunostained for MyoD were then counterstained with hematoxylin in order to highlight nuclei.

As negative controls, all primary antibodies were replaced by non-immunized specific serum.

<b>Antigen</b>	<b>Antigen unmasking</b>	<b>Primary antibody</b>	<b>Secondary antibody</b>	<b>Revelation</b>
<b><math>\alpha</math>-SMA</b>	No	1:300 30 minutes	Anti-mouse biotinylated	Vectastain <sup>®</sup>
<b>TGF-<math>\beta</math></b>	12 minutes	1:50 Overnight	Anti-rabbit 1:200	PAP 1:200
<b>CTGF</b>	No	1:200 Overnight	Anti-rabbit biotinylated 1:200	Streptavidin- HRP 1:1000
<b>PDGF-B</b>	16 minutes	1:100 Overnight	Anti-rabbit 1:100	PAP 1:200
<b>8-OHdG</b>	20 minutes	1:500 30minutes	Anti-mouse biotinylated	Vectastain <sup>®</sup>
<b>Cleaved Caspase-3</b>	20 minutes	1:300 Overnight	Anti-rabbit biotinylated 1:200	Streptavidin- APK
<b>p16<sup>ink4A</sup></b>	20 minutes	1:200 30 minutes	Anti-mouse biotinylated	Vectastain <sup>®</sup>
<b>p21</b>	15 minutes	1:300 Overnight	Anti-mouse biotinylated	Vectastain <sup>®</sup>
<b>PCNA</b>	20 minutes	1:100 30 minutes	Anti-mouse biotinylated	Vectastain <sup>®</sup>
<b>Ki-67</b>	20 minutes	1:100 Overnight	Anti-rabbit 1:200	PAP 1:200
<b>MyoD</b>	20 minutes	1:50 Overnight	Anti-mouse biotinylated	Vectastain <sup>®</sup>
<b>P2Y<sub>2</sub></b>	10 minutes	1:150 Overnight	Anti-rabbit biotinylated 1:200	Streptavidin- APK
<b>P2X<sub>4</sub></b>	5 minutes	1:100 Overnight	Anti-rabbit 1:200	PAP 1:200
<b>P2X<sub>7</sub></b>	10 minutes	1:350 Overnight	Anti-rabbit 1:200	PAP 1:200
<b>IL-6</b>	10 minutes 600W	1:300 30 minutes	Anti-mouse biotinylated	Vectastain <sup>®</sup>
<b>MMP-9</b>	8 minutes	1:400 Overnight	Anti-rabbit biotinylated 1:200	Streptavidin- HRP 1:1000

*Tab.3 Immunohistochemical Analysis*

*Statistical analysis:* Data are presented as mean  $\pm$  standard deviation. The significance of the differences was calculated using one way analysis of variance. A *p value* of less than 0,05 was considered significant.

## RESULTS:

### *Emphysema*

The entity of emphysema, quantified by using morphometric analysis, is reported in Figure 5. A light microscopy examination of the lungs harvested from C57 Bl/6J and DBA/2 mice exposed to cigarette smoke for 7 and 11 months showed significant higher values of mean linear intercepts (Lm) and significant lower values of internal surface area of lungs (ISA) when compared to mice exposed to room air of the same strain at the same time points. Data obtained confirmed the data previously observed in our laboratory.

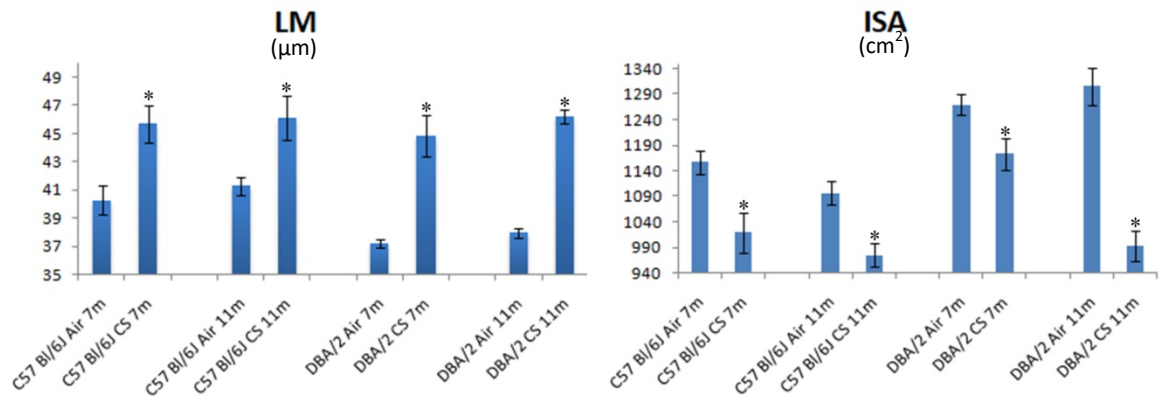


Figure 5. *Quantification of emphysema. \* p < 0.05 vs the air control of the same strain at the same time of exposure*

### *Bronchial and bronchiolar remodeling*

In order to evaluate the entity of peri-bronchiolar fibrosis, Masson's trichrome staining on tissue slides was performed. As we can see in Figure 6 (B, C, E, F) C57 Bl/6J mice show, after cigarette smoke exposure, an increased deposition of collagen (stained in light green) around bronchioles, distal and main bronchi in lung parenchyma, when slides are compared with those from control animals at the same time points (A and D). After 7 months of smoke exposure, we found only a small amount of collagen (Fig. 6B and C),

accompanied by a massive infiltration of inflammatory cells (arrowheads), that increases progressively during the following 4 months of treatment (Fig. 6E and F). No changes in morphology are seen in control mice at all age (Fig. 6A and D).

Same features are observed in air exposed and smoking DBA/2 mice. Following chronic smoke exposure, they show a marked peri-bronchial fibrosis with a progressive deposition of collagen, which is extended also near small bronchi and vessels. These lesions are not evenly distributed in the parenchyma and are more consistently present in the mice exposed to cigarette smoke for 11 months (Fig. 7E and F). DBA/2 control animals show only a faint green stain around cartilaginous bronchi (Fig. 7A and D).

Of interest, DBA/2 mice show a more consistent deposition of collagen around bronchi and bronchioles when compared to C57 Bl/6J mice at all time points reported in figures 6 and 7.

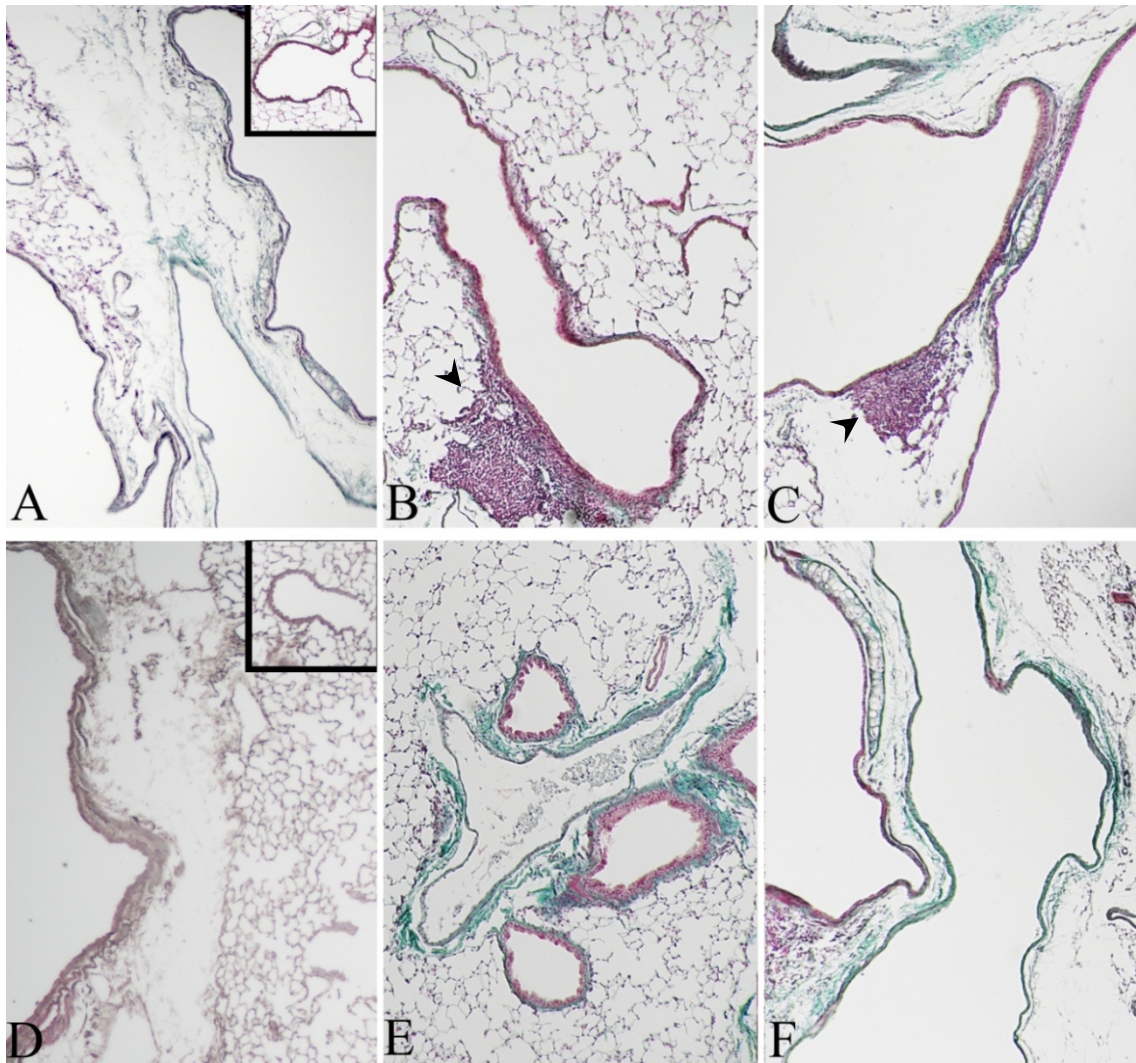
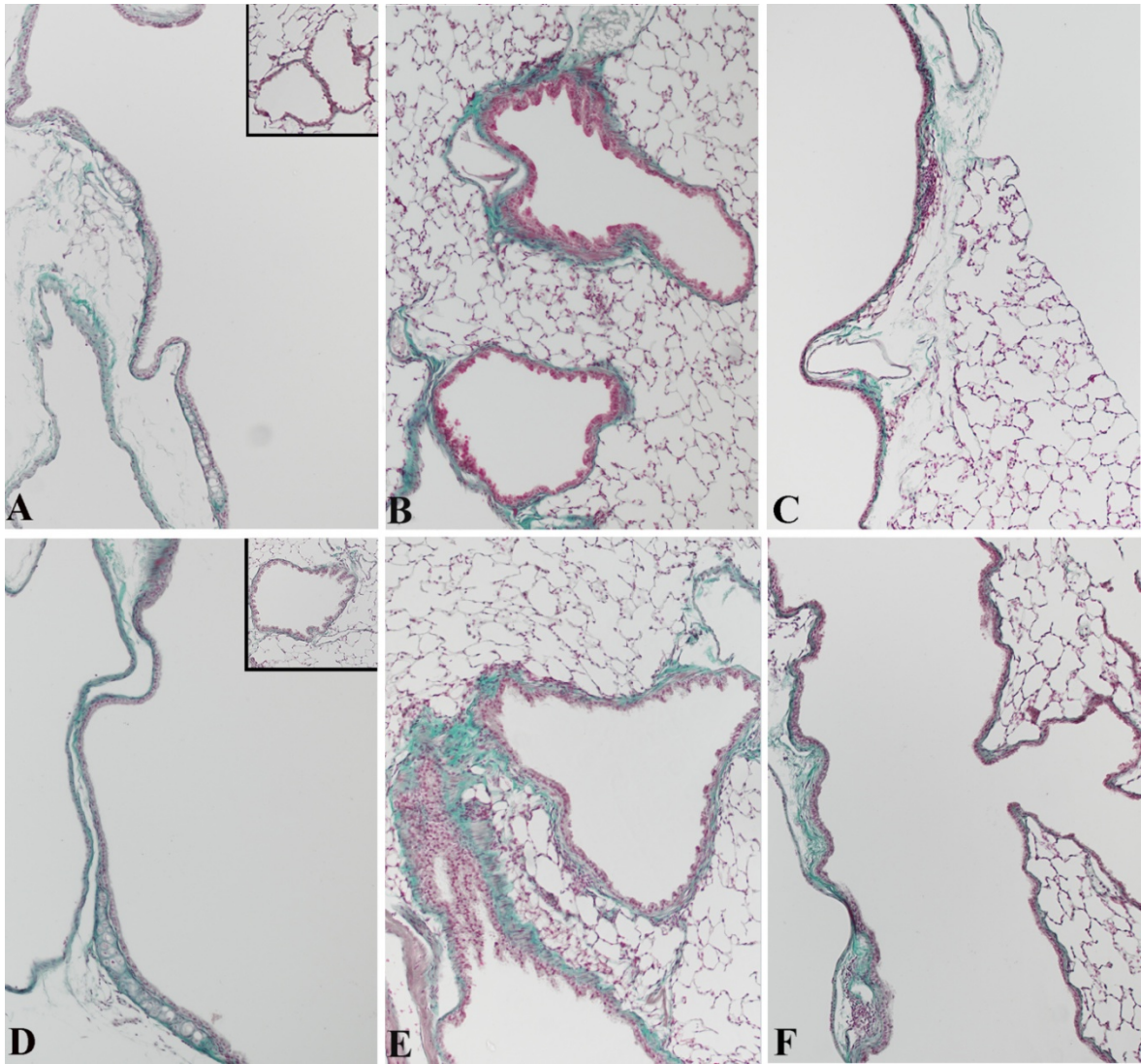


Figure 6. Airway remodeling in representative C57 Bl/6J mice pulmonary sections. (A) and (D): Large bronchi of control animals exposed to air for 7 and 11 months, respectively, are reported. (Inserts) Parenchymal section showing small bronchi and a vessel. (B) and (C) Medium and small bronchi and cartilaginous bronchus from a mouse exposed to cigarette smoke for 7 months. In (E) and (F) medium and small bronchi and a large bronchus from mice exposed to cigarette smoke for 11 months are shown. Masson's trichrome stain, Original Magnification x100.



*Figure 7. Airway remodeling in representative DBA/2 mouse pulmonary sections. (A) and (D) Large bronchi of control animal exposed to air for 7 and 11 months. (Inserts) Parenchymal sections showing small bronchi and vessel. (B) and (C) Medium and small bronchi and a large bronchus from a mouse exposed to cigarette smoke for 7 months. In (E) and (F) medium and small airways and large bronchus from a mouse exposed to cigarette smoke for 11 months are seen. Masson's trichrome stain. Original magnification x100.*

The entity of the peri-bronchiolar and bronchial remodeling was also approached by using  **$\alpha$ -SMA** immunohistochemical staining. The  $\alpha$ -smooth muscle actin ( $\alpha$ -SMA) is the actin isoform that predominates within smooth muscle cells and it is expressed also by myofibroblasts. These cells play an important role in fibrogenesis. Control mice show only a few positive stained spots (Fig. 8A and B) while mice chronically exposed to cigarette smoke for 7 (Fig. 8C and D) and 11 months (Fig. 8E and F) show thicker layers of  $\alpha$ -SMA positive cells, which progressively increase with time and circled main (not shown), distal bronchi and small vessels (Fig. 8G, H, I, and J). It is interesting to note that DBA/2 mice show a more evident intensity of  $\alpha$ -SMA reaction from 7 months onward. Additionally, the presence of  $\alpha$ -SMA positive cells is widely distributed in airways and intraparenchymal vessels in respect to C57 Bl/6J mice. In the latter strain  $\alpha$ -SMA positive cells are unevenly distributed throughout lung parenchyma.

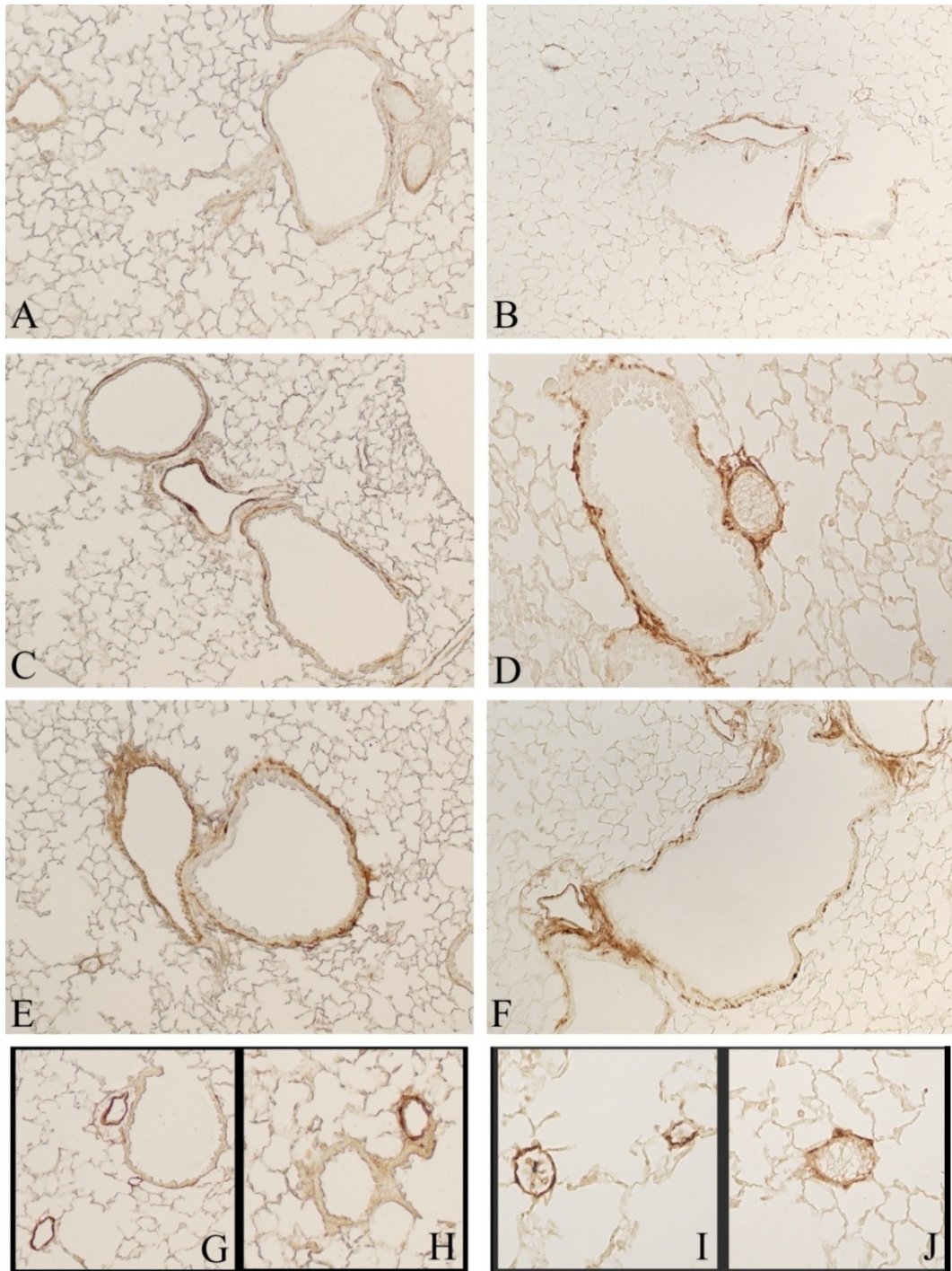


Figure 8. Representative pulmonary sections stained for  $\alpha$ -SMA. (A) and (B) Tissue sections from C57 Bl/6J and DBA/2 control mice exposed to room air. (C) and (D) Small airways and vessels from C57 Bl/6J and DBA/2 mice, respectively, exposed to cigarette smoke for 7 months. (E) and (F) Small bronchi and vessels from C57 Bl/6J and DBA/2 mice, respectively, exposed to cigarette smoke for 11 months. (G) and (H) Intraparenchymal vessels of C57 Bl/6J mouse exposed to cigarette smoke for 11 months. (I) and (J) Intraparenchymal vessels of DBA/2 mouse exposed to



*cigarette smoke for 11 months. (A-F) original magnification x100; (G-J) original magnification x200.*

### ***Goblet cell Metaplasia***

Goblet cell metaplasia (GCM) was evaluated after PAS staining of tissue slides. In Figure 9, lung representative sections of a C57 Bl/6J air-control (A) and of a mouse exposed to cigarette smoke (B) are reported. As can be seen there is a clear difference between control and smoker mice. Additionally, we found no appreciable difference between air-controls, as well as between smoking mice within this mouse strain at 7, when 75% of mice develop GCM), and 11 months of exposure (70%). After chronic exposure to cigarette smoke, C57 Bl/6J mice develop a goblet cell metaplasia both in large and small airways (Fig. 9B).

Of interest, DBA/2 mice show only a few goblet cells at 7 months of cigarette smoke exposure that are localized mainly in the large bronchi (Fig. 10C). A more consistent goblet cell metaplasia is detected after 11 months of exposure. At this time point, PAS positive cells can be seen in large bronchi (Fig. 10F) and also in some small bronchi (Fig. 10E) even if only 35% of animals of this strain develop GCM. Control animals show no positively stained PAS cells at any time (Fig. 10A and D).

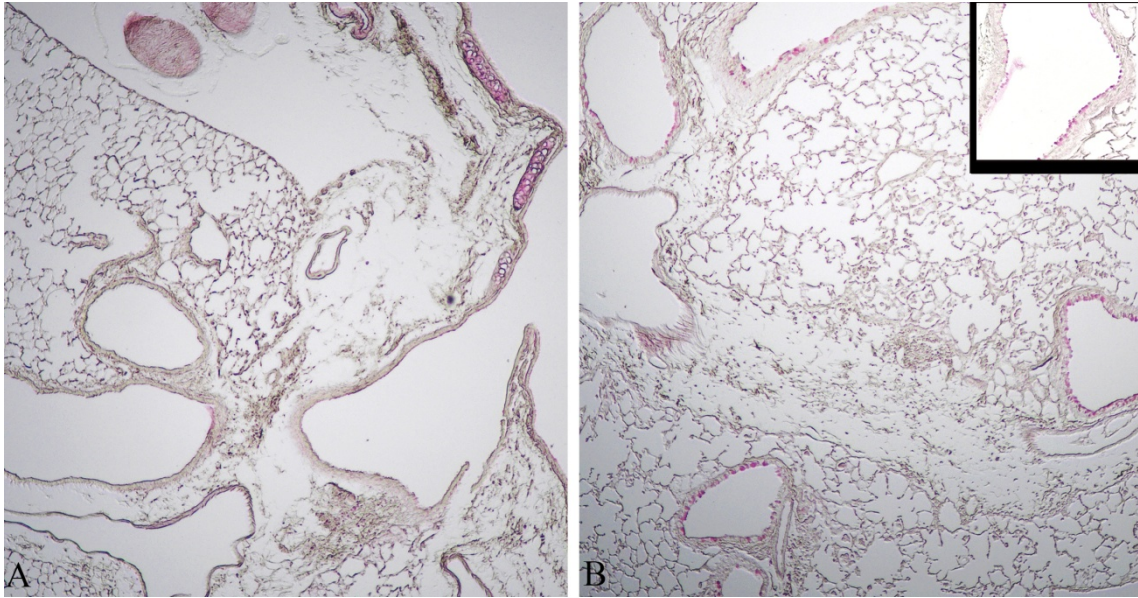


*Figure 9. PAS staining of C57 Bl/6J pulmonary sections (A): Representative section from air-control mouse. (B): Small airways of smoke exposed mouse. (Insert) large bronchus of a mice exposed to chronic cigarette smoke for 11 months. Original magnification x40.*

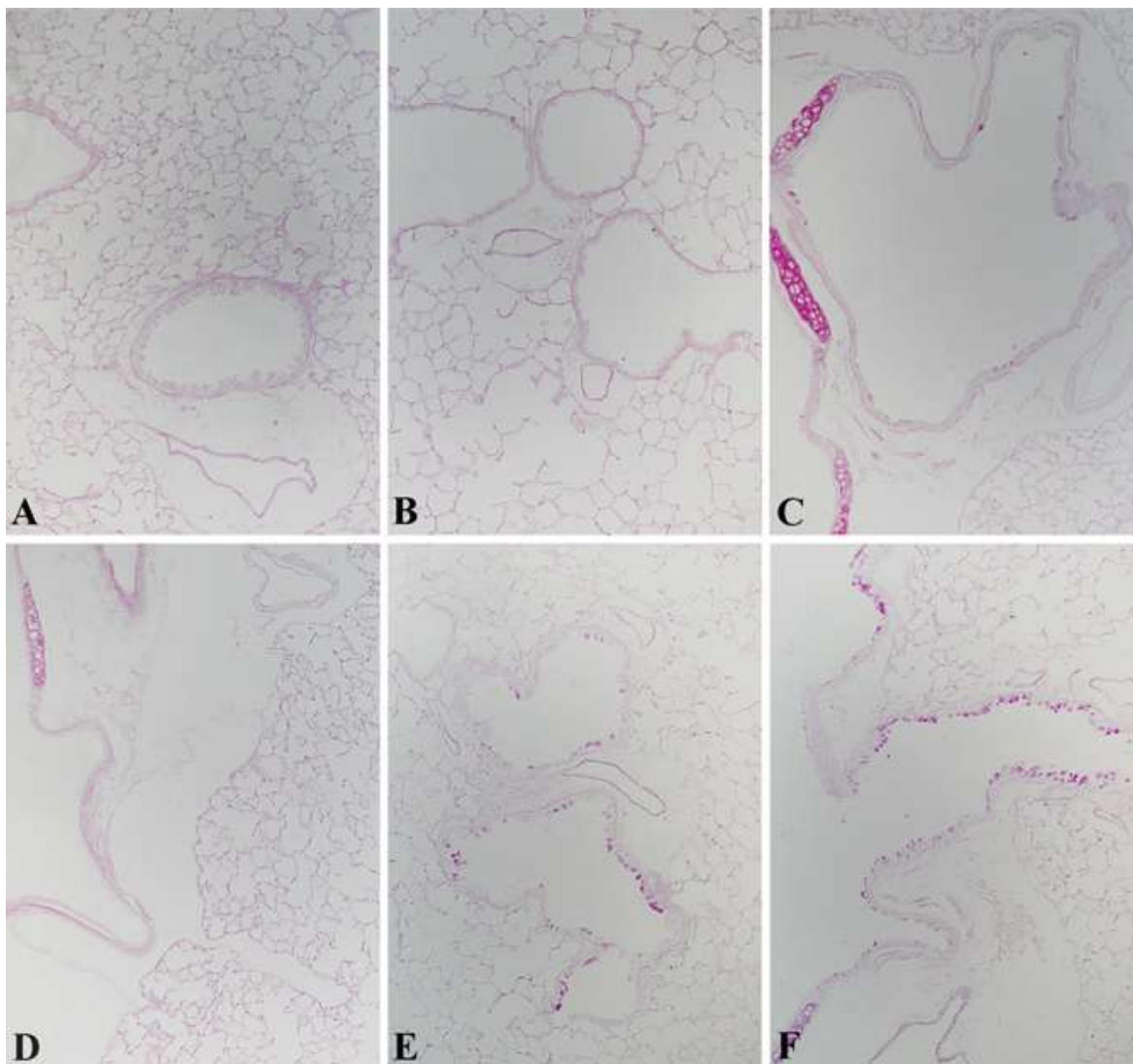


Figure 10. PAS staining of DBA/2 mice pulmonary sections.

(A) and (D) are representative sections of DBA/2 control mice exposed to room air. In (B) and (C) small intra-parenchymal airways and small vessels, and large airways of mice exposed to cigarette smoke for 7 months are reported. (E) and (F) bronchioles, vessels, and a cartilaginous bronchus from mice exposed to cigarette smoke for 11 months are shown. Original magnification x100.

### ***Growth factors expression***

Several growth factors were analyzed in order to investigate mechanism(s) underlying the remodeling associated with smoke induced COPD. **TGF- $\beta$**  expression was evaluated and an increased level of the growth factor is appreciated in main and small bronchi of both C57 Bl/6J (Fig. 11B and C) and DBA/2 (Fig. 11E and F) smoking mice. A faint reaction is seen in control mice (Fig. 11A and D) at the examined time points. In inserts of Figure 11, a positive stain of the muscular layer is appreciable beneath the bronchial epithelium.

**CTGF** expression showed a different pattern between the two mouse strains, and at the various examined times. A progressive increase in stain positivity is seen in C57 Bl/6J mice at 7 months of exposure (Fig. 12C), (when the expression is localized mostly in bronchiolar epithelium) and at 11 months of exposure (Fig. 12E). At 11 months, CTGF expression is localized in epithelial cells as well as in the muscular layers that circle bronchioles and vessels (Fig. 12G and H). No positive stain is appreciated in control mice (Fig. 12A).

On other hand, DBA/2 mice showed no appreciable difference in CTGF expression around parenchymal bronchioles at 7 and 11 months of smoke exposure (Fig. 12D and F). We observe higher expression of this fibrogenic cytokine in smoking mice when compared with that present in control ones (Fig. 12B). An increased expression of CTGF is seen in the muscular layer of large airways (Fig. 12I) and in small vessels (Fig. 12H) of DBA/2 mice after 11 months of smoke exposure.

Finally, **PDGF-B** expression is highly increased in intra-parenchymal airways of C57 Bl/6J mice after 7 months exposure to cigarette smoke (Fig. 13B). After 11 months of exposure, a significant decrease of PDGF-B expression is seen in small bronchi (Fig. 13C). However, it remains expressed mostly in airways and vessel smooth muscle cells (Fig.

13C, arrowheads) and inflammatory cells (Fig. 13B and C, arrows). On the other hand, DBA/2 mice showed a comparable PDGF-B expression in large and small airways at 7 (Fig. 13E) and 11 months (Fig. 13F) of exposure.

Only a faint positivity can be seen in lung sections of control mice (Fig. 13A and D).

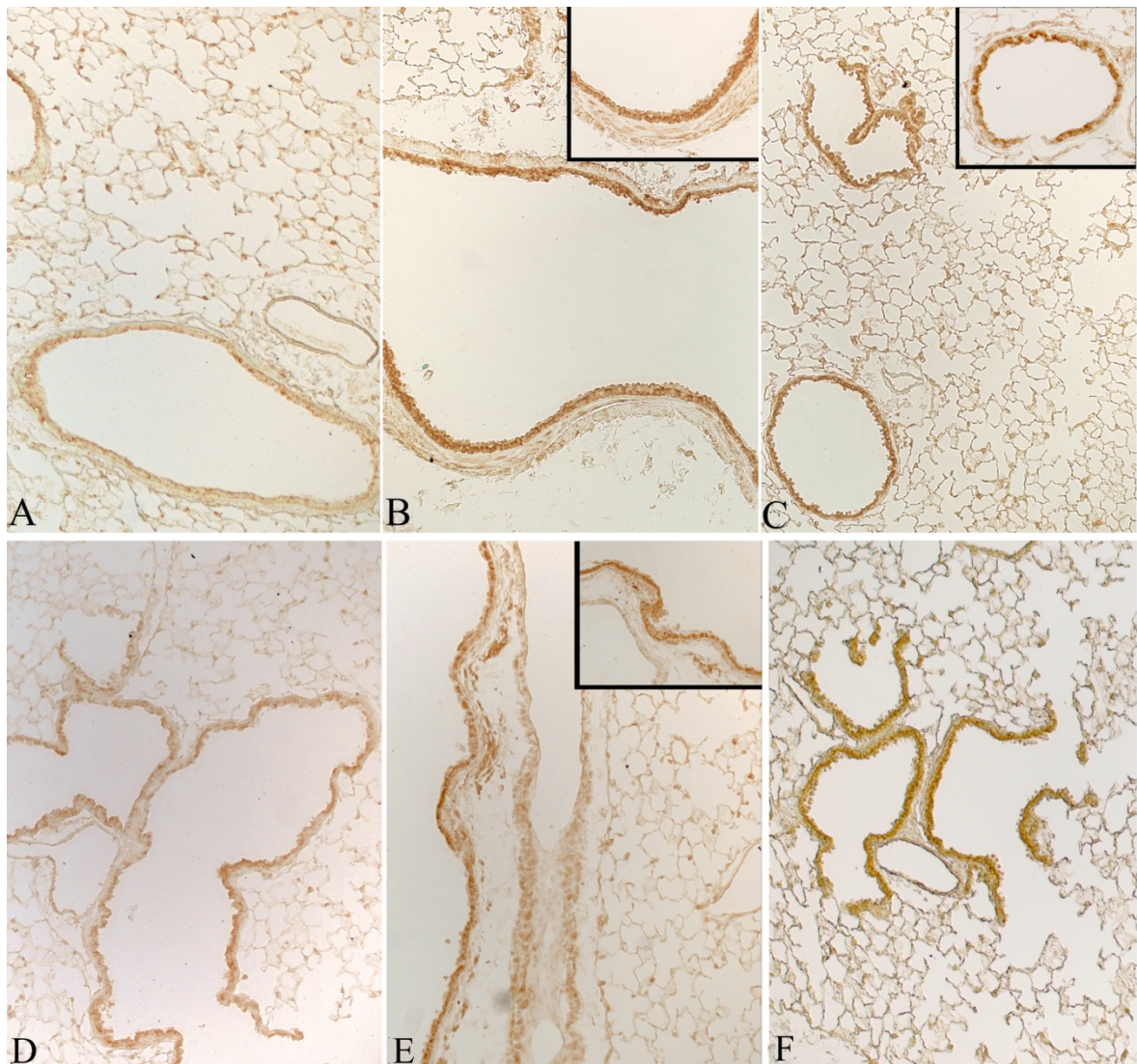


*Figure 11. Immunohistochemical reaction for TGF- $\beta$  on representative tissue section of C57 Bl/6J mice (A) and DBA/2 mice (D) exposed to room air. In (B) and (C) a representative section of large airway and parenchymal bronchioles of C57 Bl/6J mice exposed to chronic cigarette smoke is shown. In (E and F) Cartilaginous bronchus, small airways and intraparenchymal vessel of DBA/2 mice exposed to cigarette smoke are reported. (A-F) original magnification x100. (Inserts)*

show a higher magnification (x200) which better highlight the positive staining on the muscle layer under the bronchiolar epithelium.

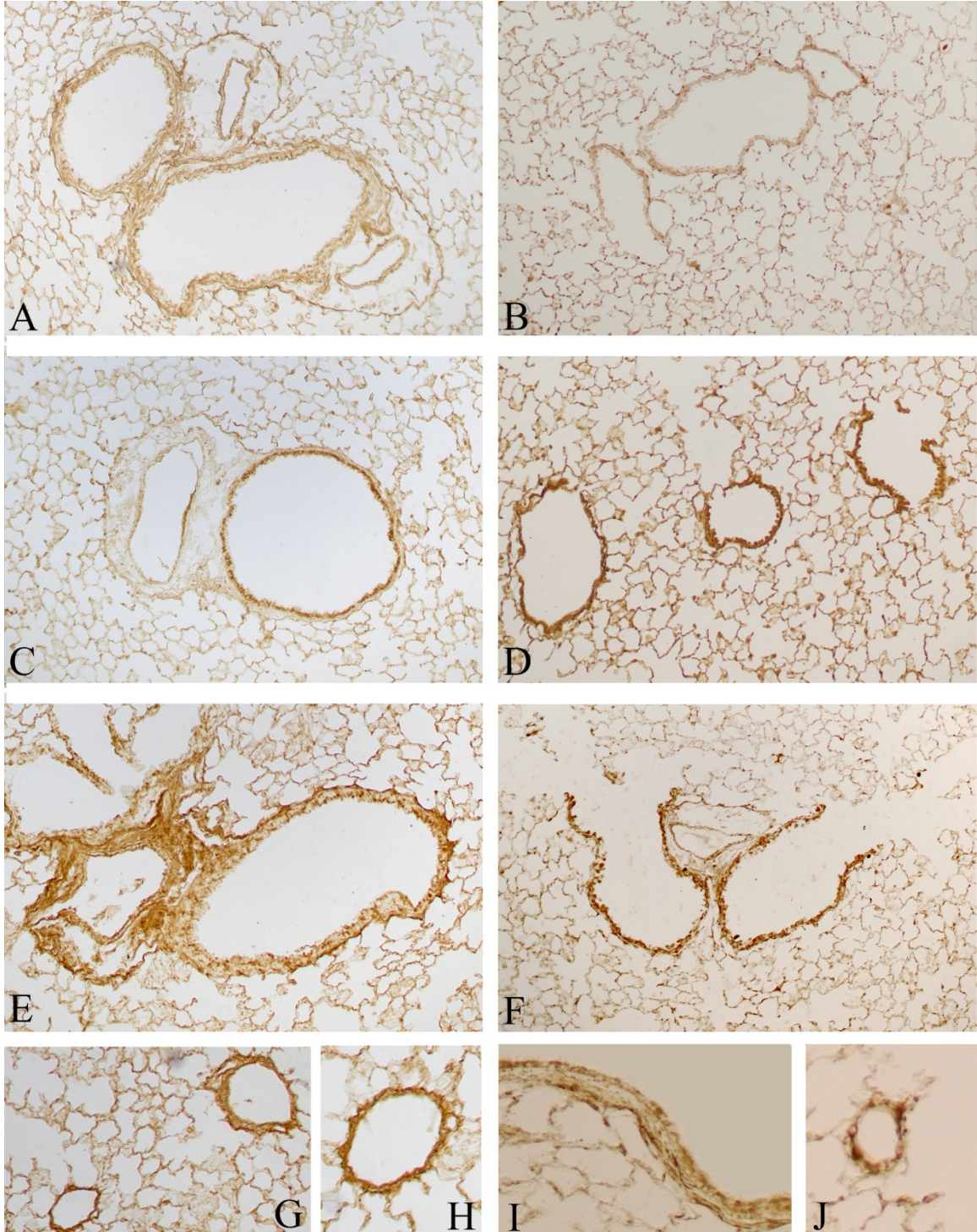
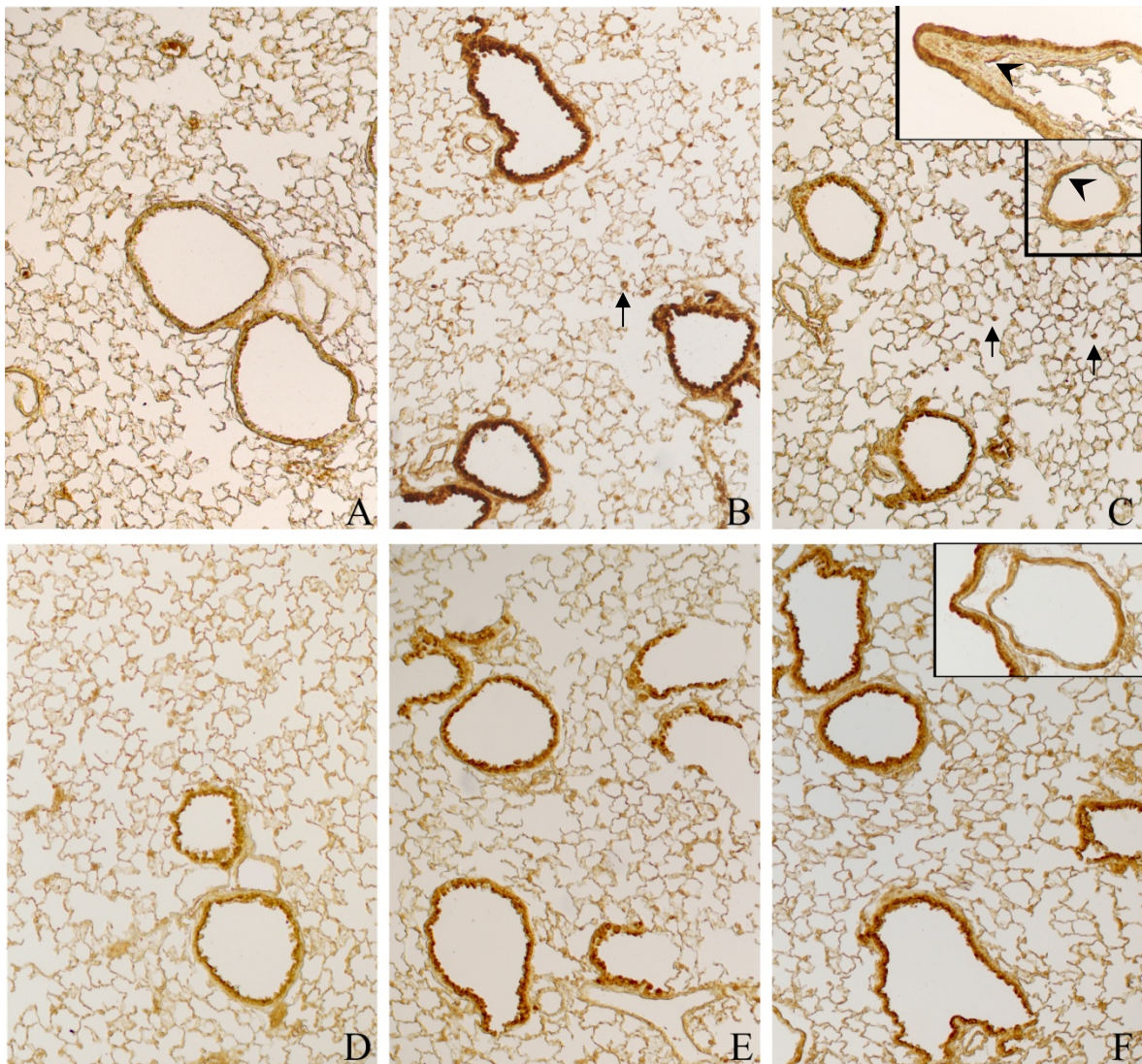


Figure 12. Immunohistochemical reaction for CTGF. (A) and (B) report control sections of C57 BL/6J mice and DBA/2 mice, respectively. Intraparenchymal bronchioles of C57 BL/6J (C) and

*DBA/2 mice (D) exposed to cigarette smoke for 7 months are shown. Intraparenchymal bronchioles of C57 Bl/6J (E) and DBA/2 mice (F) exposed to cigarette smoke for 11 months. Small vessels from C57 Bl/6J (G and H) and DBA/2 mice (J), as well as a large airway from a DBA mouse (I) exposed cigarette smoke for 11 months are shown. (A-G) original magnification x100. (H-J) original magnification x200.*



*Figure 13. Immunohistochemical reaction for PDGF-B. Representative sections of mouse lungs from room air exposed (A) and cigarette smoke exposed C57Bl/6J mice for 7 (B) and 11 months (C). Arrowheads indicate smooth muscle cells; arrows point to inflammatory cells. Representative lung sections from a control DBA/2 (D) and cigarette smoke exposed mice at 7 (E) and 11 months (F). (A-F) original magnification x100. (Inserts) magnification x200.*

### ***Immunohistochemical stain for 8-oxo-7,8-dihydro-2'-deoxyguanosine (8-OHdG)***

Previous work carried out by our laboratory suggested a different sensitivity to oxidative stress for C57 Bl/6J and DBA/2 mice that may condition parenchymal and airway changes induced by cigarette smoke. In order to evaluate the oxidative damage of DNA induced by chronic smoke we perform an immunohistochemical stain for 8-oxo-7,8-dihydro-2'-deoxyguanosine (8-OHdG). After 4 months of cigarette smoke exposure, an increased positivity for 8-OHdG is appreciated on nuclei of parenchymal (Fig. 14B and D) and bronchiolar cells (Fig. 15B and D). In Fig.14A and D, and Fig.15A and D, tissue slides from control mice after 8-OHdG staining are reported. Of interest, also fibroblasts, myofibroblasts and SMC are damaged by oxidants in cigarette smoke groups (Fig. 15B and D, arrow heads). Moreover, the proportion of staining nuclei is more consistent in DBA/2 (Fig. 14D and Fig. 15D) if compared to C57 Bl/6J smoking mice (Fig. 14B and Fig. 15B).

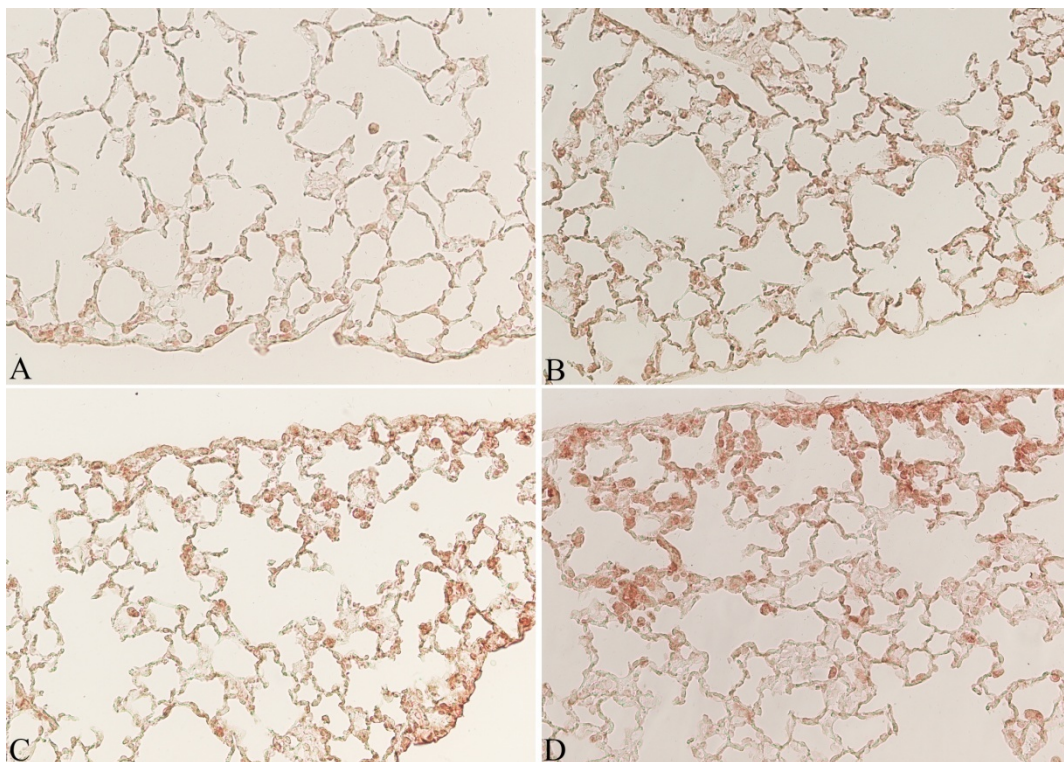


*Figure 14. Immunohistochemical reaction for 8-OHdG. Representative sections of lungs from room air (A) and cigarette smoke exposed (B) C57Bl/6 mice at 4 months. Representative sections of*



lungs from room air (C) and cigarette smoke exposed (D) DBA/2 at 4 months. Original magnification x200.

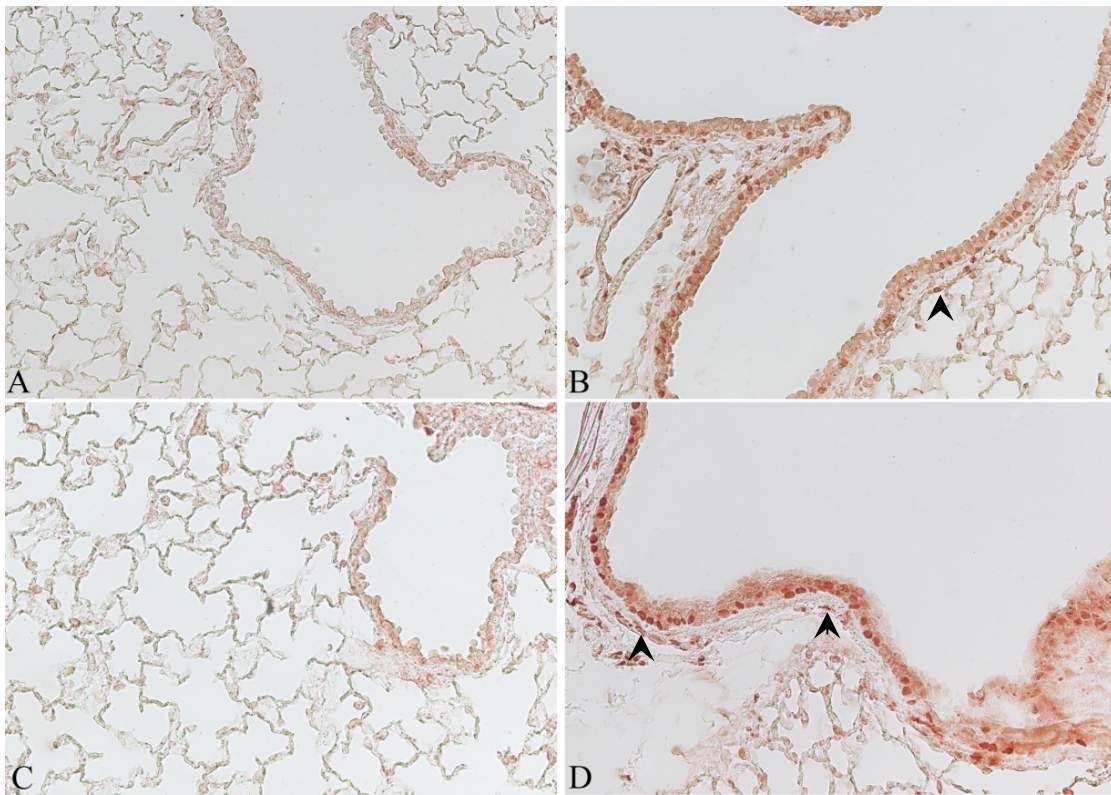


Figure 15. Immunohistochemical reaction for 8-OHdG. Representative sections of bronchi from room air (A) and cigarette smoke exposed (B) C57Bl/6J mice at 4 months. Representative sections of bronchi from room air (C) and cigarette smoke exposed(D) DBA/2 mice, at 4 months are shown. Arrowheads in (B) and (D) point to cells of the fibro-muscular layer. Original magnification x200.

Oxidative damage to DNA may lead cells to different consequences: repair, apoptosis and cellular senescence associated with apoptosis resistance. Both apoptosis and cellular senescence are suggested to participate in the pathogenesis of the morphological changes associated with COPD.

### ***Immunohistochemical stain for Cleaved Caspase-3***

**Apoptosis** has been evaluated by examining **cleaved caspase-3** immunostaining in pulmonary tissue slides. In C57 Bl/6J control mice only a few positive stained cells in patchy areas are seen in bronchial and bronchiolar epithelial cells and in the subepithelial layer, and no positive stained cells are appreciated in lung parenchyma (Fig. 16A and B). After 7 months of cigarette smoke exposure, massive increase in cells positivity in lung parenchyma (Fig. 16D) is seen, that seems to be related with the increased extent of emphysema observed. At this time, an almost absent positivity is seen in sub-bronchiolar fibro-muscular layer (Fig. 16C). At 11 months of exposure, cleaved caspase-3 is absent around bronchi and its positivity is decreased in lung parenchyma. This suggests that oxidative damage in C57 Bl/6J mice occurs at the maximal extent between 7 and 11 months of smoke exposure.

DBA/2 mice show a similar immunohistochemical pattern in lung parenchyma, where no positive cells in control mice are found (Fig. 17B) but a widespread positivity for caspase-3 is detected after 7 months exposure to cigarette smoke (Fig. 17D). Of interest, DBA/2 mice show an increased expression of cleaved caspase-3 also in epithelial bronchial cells after 7 months exposure (Fig. 17C) when compared with control animal (Fig. 17A).

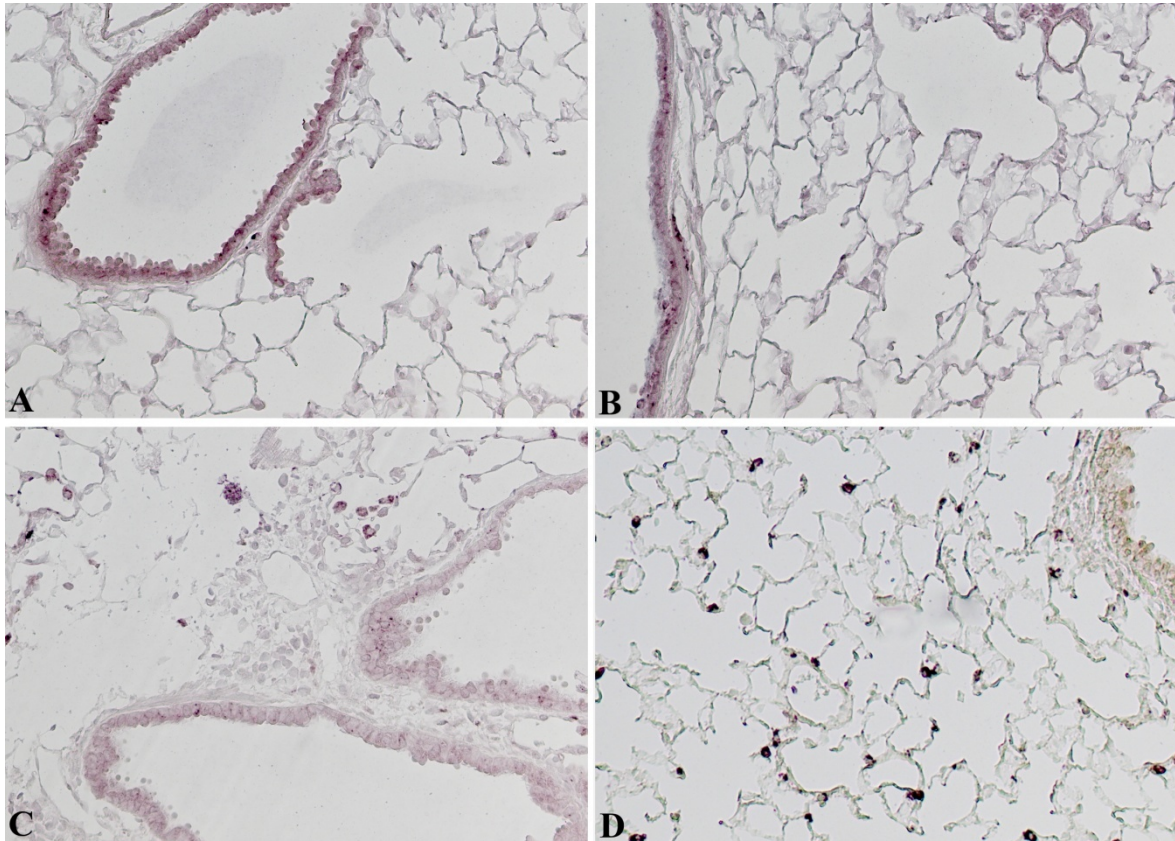


Figure 16. Immunohistochemical staining for Cleaved caspase-3. Representative sections of pulmonary tissue of C57 Bl/6J mice. (A) Intraparenchymal bronchus and (B) lung parenchyma of control mouse. Intraparenchymal bronchi(C) and lung parenchyma (D) of 7 months smoking mouse. Original magnification x200.

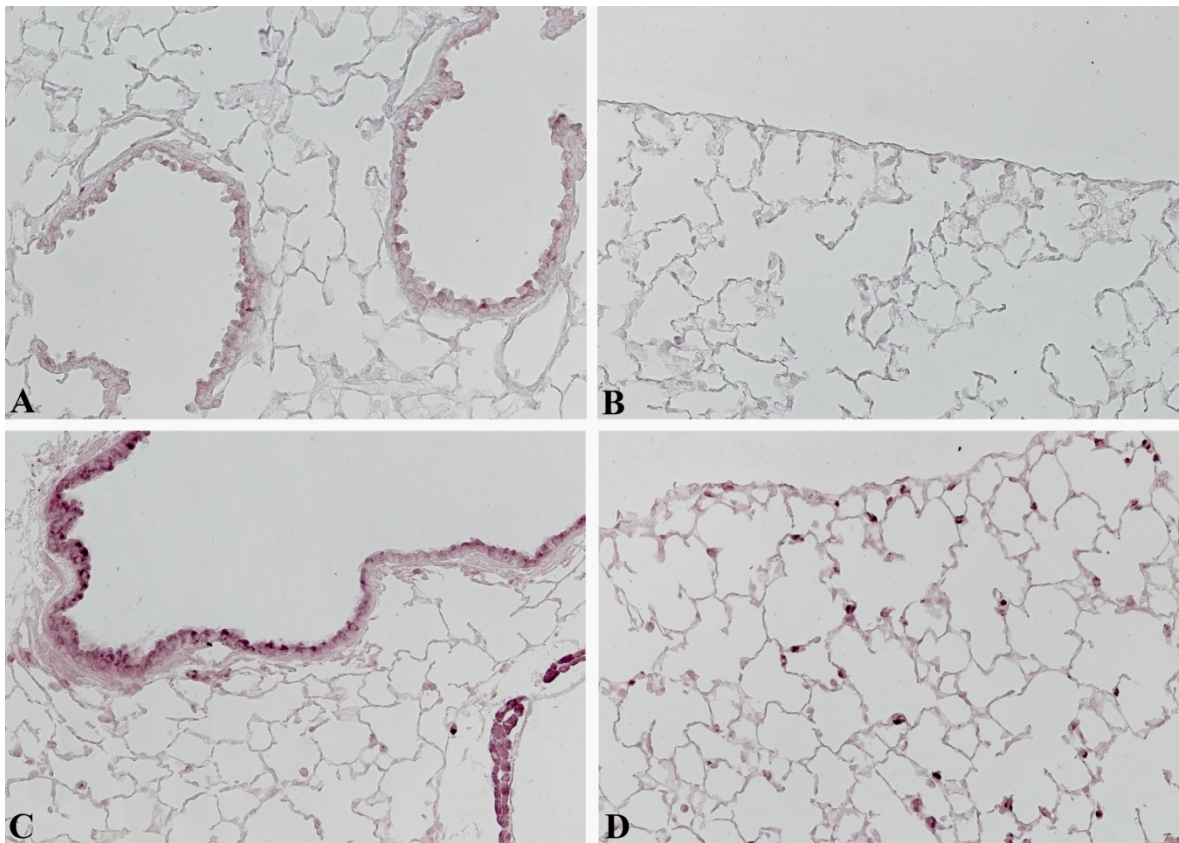


Figure 17. Immunohistochemical staining for Cleaved caspase-3. Representative sections of the pulmonary tissue of DBA/2 mice. (A) Intra-parenchymal bronchus and (B) lung parenchyma of control mouse. Intra-parenchymal bronchi (C) and parenchyma (D) of 7 months smoking mouse. Original magnification x200.

#### **Immunohistochemical stain for p16<sup>ink4A</sup>**

p16<sup>ink4A</sup> immunohistochemistry was performed in order to evaluate cellular senescence induced by cigarette smoke. The absence of p16<sup>ink4A</sup> positivity in C57 Bl/6J mice exposed to room air for 1 month (Fig. 18A) indicate that no cellular senescence is induced in these mice at this time point. Additionally, only a few positive cells are seen in mature mice of the same strain exposed to room air for 11 months (Fig. 18B).

It is interest to note that after 4 months of exposure to cigarette smoke an increase in cell positivity for p16<sup>ink4A</sup> is found in bronchial epithelial cells, fibroblasts, and myofibroblasts

localized in the sub-epithelial layer (Fig. 18C) and lung alveolar type II cells (Fig. 18D, arrows). DBA/2 mice show a similar p16<sup>ink4A</sup> staining pattern in lung parenchyma after 4 month of smoke exposure (Fig. 19D), while a more marked staining is found in bronchiolar epithelial cells after 4 months of exposure (Fig. 19C) when it is compared to that observed on bronchi of C57 Bl/6J mice (Fig. 18C). Only a faint staining is appreciable in pulmonary sections of control mice (Fig. 19A and B). p21 immunohistochemistry has been also performed in order to evaluate cellular senescence. The pattern of expression of p21 observed in pulmonary cells confirmed that seen for p16<sup>ink4A</sup> (data not shown).

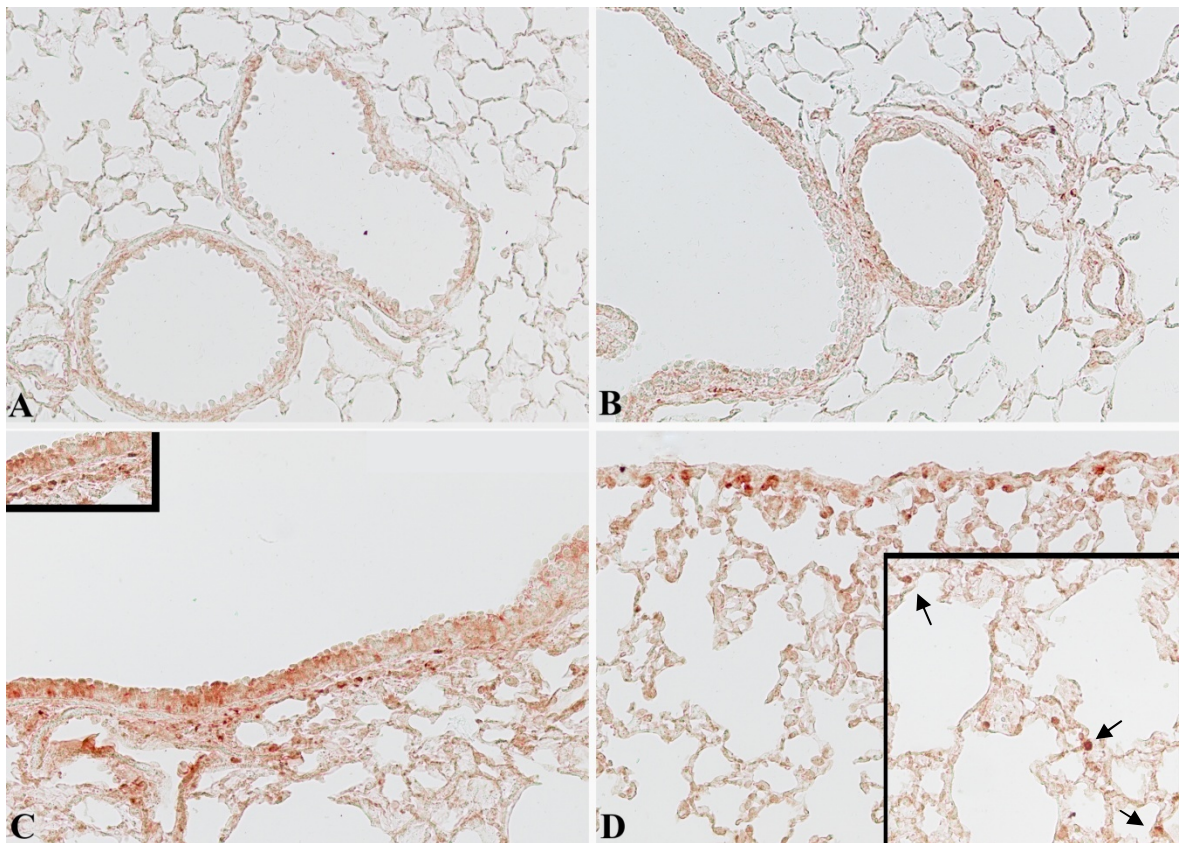


Figure 18. Immunohistochemical staining for P16<sup>ink4A</sup> on representative sections of C57 Bl/6J mice. (A) and (B) depict bronchi and lung parenchyma of a mouse exposed to room air for 1 month and 11 months, respectively. (C) and (D) depict bronchi and lung parenchyma from a mouse exposed to cigarette smoke for 4 months. Arrows in (D) point to alveolar type II cells. Original magnification x200; insert in (C) magnification x400.

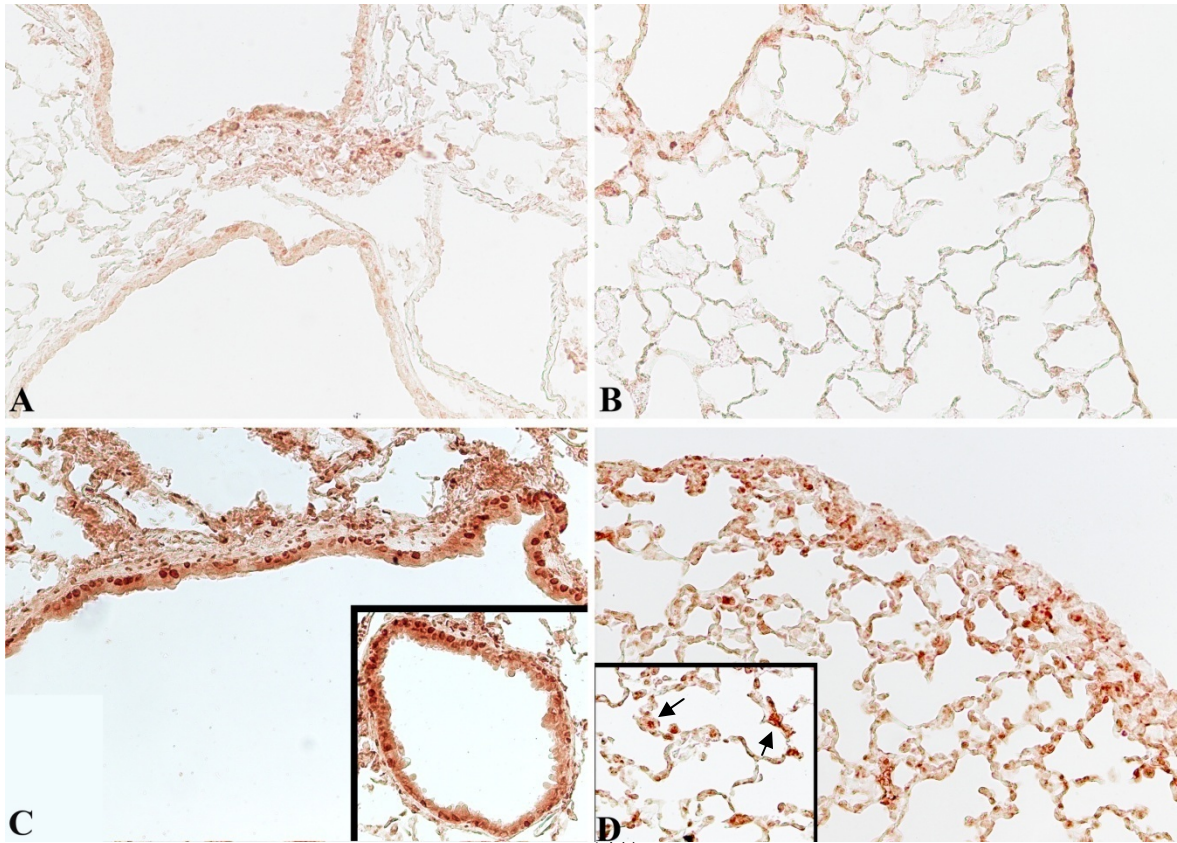


Figure 19. Immunohistochemical staining for P16<sup>ink4A</sup> on representative sections of DBA/2 mice. In (A) and (B) bronchi and lung parenchyma of a mouse exposed to room air for 1 month and 11 months, respectively, are shown. (C) and (D) show bronchi and lung parenchyma from a mouse exposed to cigarette smoke for 4 months. Arrows in (D) point to alveolar type II cells. Original magnification x200.

### ***Immunohistochemical stain for Proliferating Cell Nuclear Agent (PCNA)***

Finally, we evaluated cell proliferation through an immuno-localization in pulmonary tissue of PCNA. Only a few number of cells are positive for PCNA stain in lung sections of air-control mice from C57 Bl/6J (Fig. 20A) and DBA/2 (Fig. 20C) strains. However, after cigarette smoke exposure for 4 months both strains show in lung cells an increased number of nuclei positive for PCNA. A more pronounced increase is observed in C57 Bl/6J bronchial cells (Fig. 20B) than in DBA/2 ones (Fig. 20D). In DBA/2 mice the greatest increase in positive cells is localized in the sub-bronchiolar fibro-muscular layer (Fig. 20D) and in the subpleural areas (Fig. 20F), whereas in C57 Bl/6J mice a low number

of proliferating cells is present in the subpleural areas (Fig. 20E). PCNA staining was sided by an immunostaining for Ki-67 (not shown), which confirmed the same pattern of positivity we observe with PCNA.

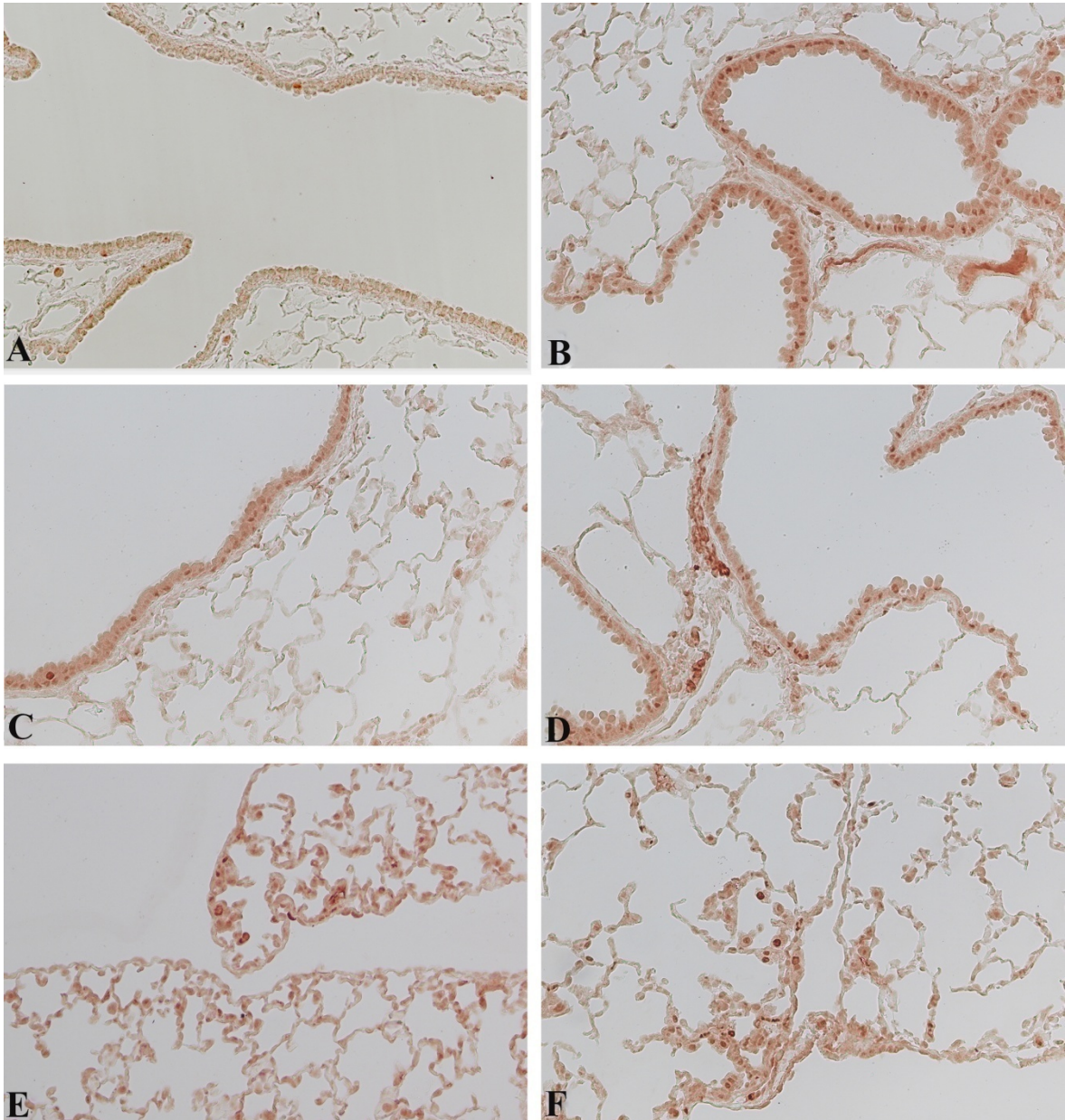
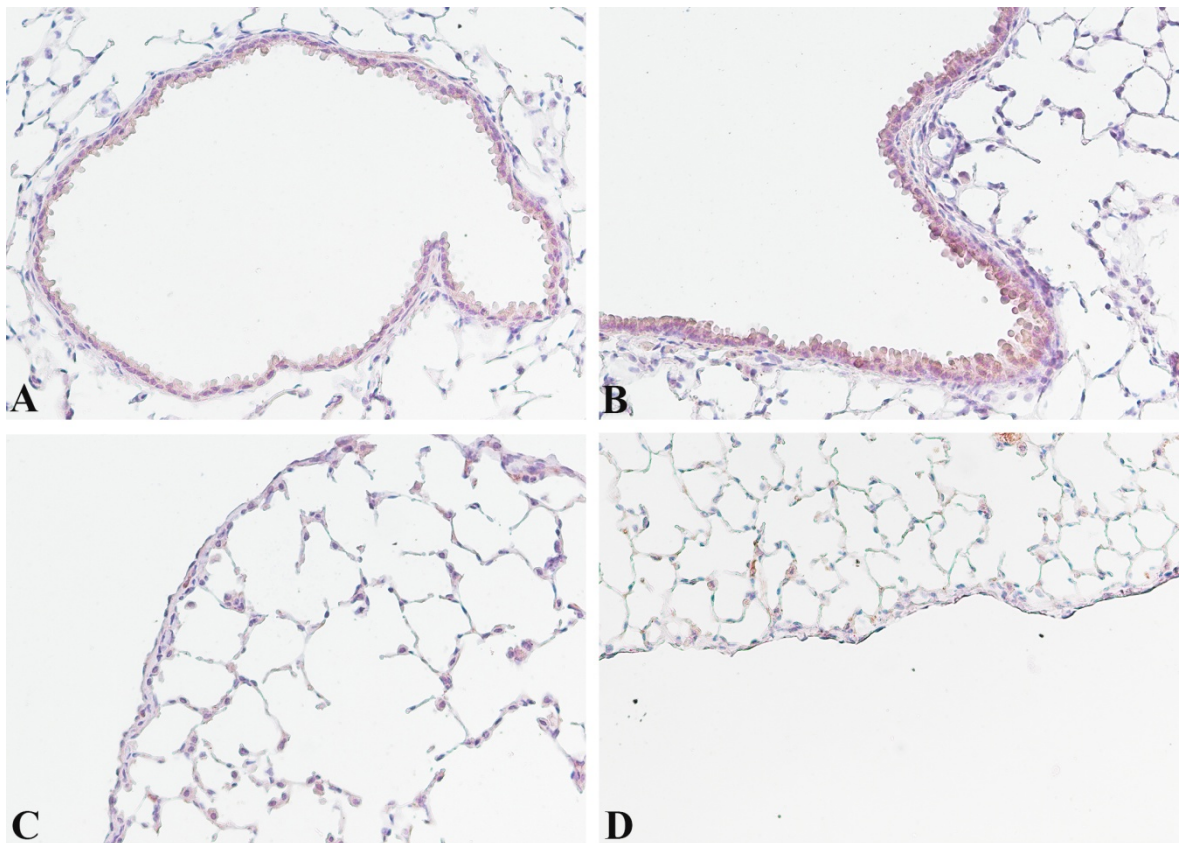


Figure 20. Immunohistochemical stain for PCNA. (A) and (C) report control sections of C57 Bl/6J and DBA/2 mice, respectively. Lung section of C57 Bl/6J (B) and DBA/2 mice (D) exposed to cigarette smoke for 4 months are shown. Sub-pleural areas of C57 Bl/6J (E) and DBA/2 mice (F) exposed to cigarette smoke for 4 months. (A-E) original magnification x200.

### ***Immunohistochemical staining for MyoD***

MyoD is a transcription factor which plays a critical role in myogenic differentiation and its expression has been associated with myofibroblasts presence in tissue repair/fibrosis. In control animals no MyoD expression can be seen in bronchioles and subpleural areas of both C57 Bl/6J (Fig. 21A and C) and DBA/2 strains (Fig. 22A and C). An appreciable increase in MyoD expression is detectable in DBA/2 mice exposed to cigarette smoke for 4 months in sub-bronchiolar fibro-muscular layer (Fig. 22B) as well as in subpleural areas (Fig. 22D). No positive cells to MyoD stain can be appreciated in C57 Bl/6J bronchi (Fig. 21B) and only a few in subpleural areas (Fig. 21D).



*Figure 21. Immunohistochemical staining for MyoD counterstained with hematoxylin on representative sections of C57 Bl/6J mice. (A) and (C) depict bronchi and lung parenchyma of a mouse exposed to room air for 4 months. (B) and (D) depict bronchi and lung parenchyma from a mouse exposed to cigarette smoke for 4 months. Original magnification x200.*



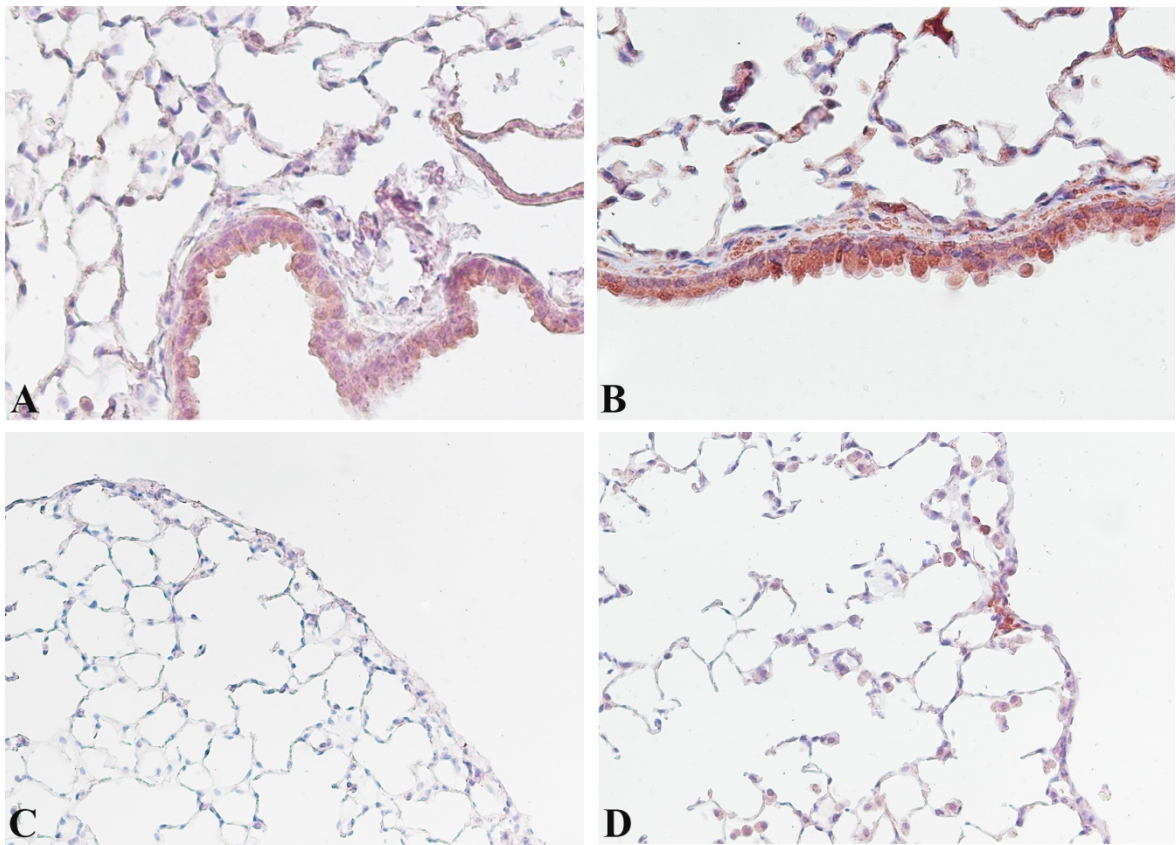


Figure 22. Immunohistochemical staining for MyoD counterstained with hematoxylin on representative sections of DBA/2 mice. (A) and (C) depict bronchi and subpleurical area of a mouse exposed to room air for 4 months. (B) and (D) depict bronchi and subpleurical area from a mouse exposed to cigarette smoke for 4 months. Original magnification x200.

### ***Purinergic Receptors***

ATP signaling has been implicated in the pathogenesis of anatomic lesions associated with COPD. Therefore, the expression of P2X<sub>4</sub> and P2Y<sub>2</sub> has been evaluated in both strains of mice after chronic exposure to cigarette smoke.

**P2Y<sub>2</sub>** expression seems to be slightly increased in C57 Bl/6J mice exposed to cigarette smoke for 7 (Fig. 23B) and 11 months (Fig. 23C) if compared to control mice (Fig. 23A). The increased expression is localized mostly on large and small airways epithelial cells and in lung parenchyma with no appreciable difference between the time points we examined. Of interest, DBA/2 mice show a different pattern of expression. Only few bronchiolar cells show a positive staining for P2Y<sub>2</sub> in control mouse (Fig. 23D) and a strong increase in positivity is seen in lung tissues from mice exposed to cigarette smoke for 7 months (Fig. 23E). After 11 months of CS exposure the positive cells for P2Y<sub>2</sub> immunostaining are decreased (Fig. 23F) when compared to those that tested positive at 7 months. However, their numbers remain increased in respect to those observed control mice.

The expression of **P2X<sub>4</sub>** is constitutively present at low levels in C57 Bl/6J (Fig. 24A) and DBA/2 mice (Fig. 24B) in large and small airways. After chronic exposure to cigarette smoke, C57 Bl/6J mice show an up-regulation of P2X<sub>4</sub> that is comparable at 7 (Fig. 24C) and 11 months (Fig. 24E) of exposure. At 7 months, DBA/2 mice show a positive reaction especially in large airways (Fig. 24D). Up-regulation of P2X<sub>4</sub> in bronchioles of DBA/2 mice is seen after 11 months from the beginning of the exposure (Fig. 24F).

An increase in P2X<sub>4</sub> and P2Y<sub>2</sub> is seen also in immune cells after cigarette smoke exposure in both strains.

The immunohistochemical staining for P2X<sub>7</sub> confirmed data previously obtained in our laboratory where P2X<sub>7</sub> expression is mainly increased, after chronic exposure to cigarette smoke, on macrophages, neutrophils and lung tissue both at 7 and 11 months (data not shown).

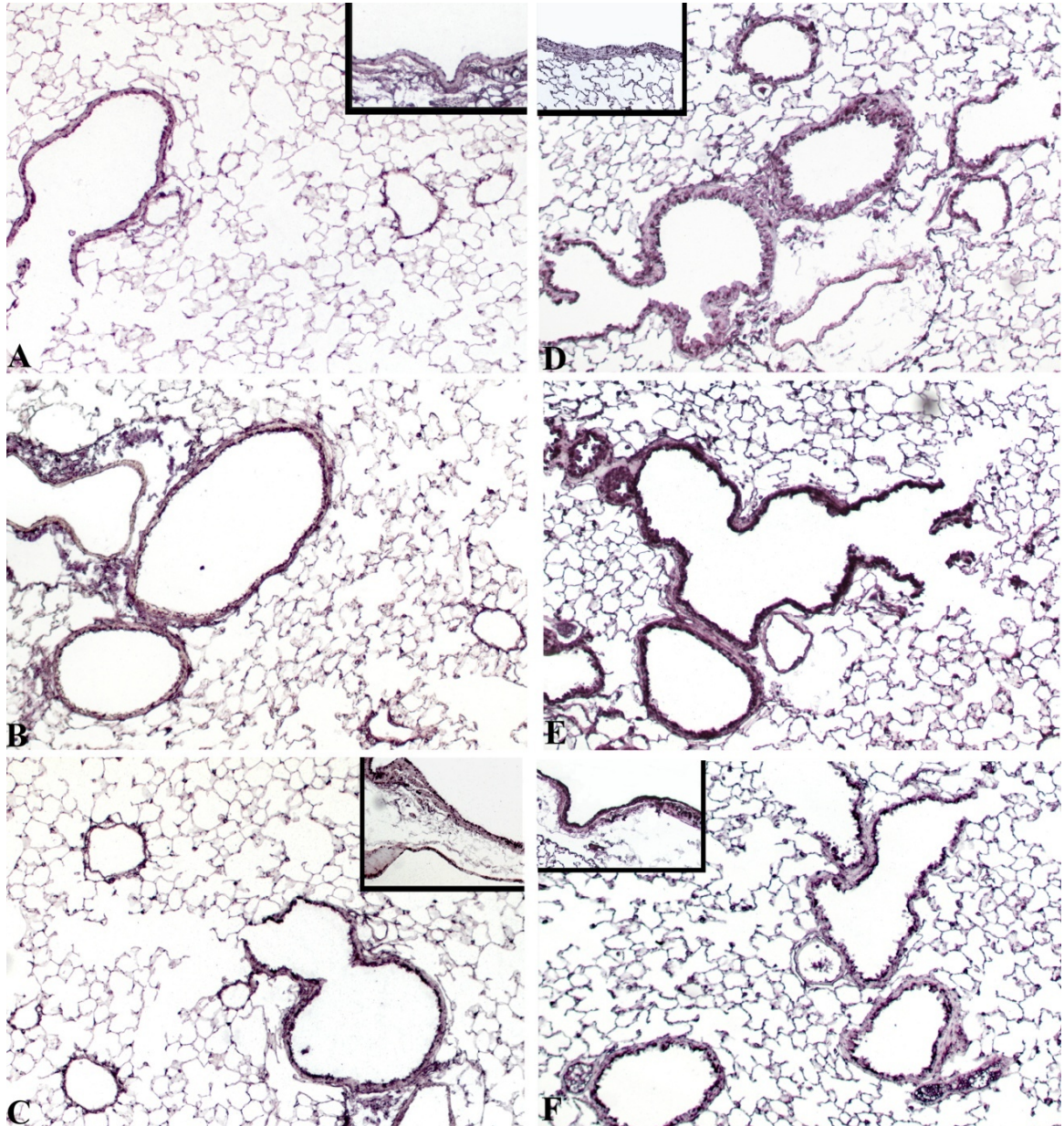


*Figure 23. Immunohistochemical staining for P2Y<sub>2</sub> on representative mouse sections of pulmonary tissue. (A) and (D) C57 Bl/6J and DBA/2 mice exposed to room air. In (B) and (E) C57 Bl/6J and DBA/2 mice exposed to cigarette smoke for 7 months are shown, respectively. (C) and (F) are*

sections from C57 Bl/6J and DBA/2 mice exposed to cigarette smoke for 11 months. Original magnification x100. (Inserts) original magnification x200.

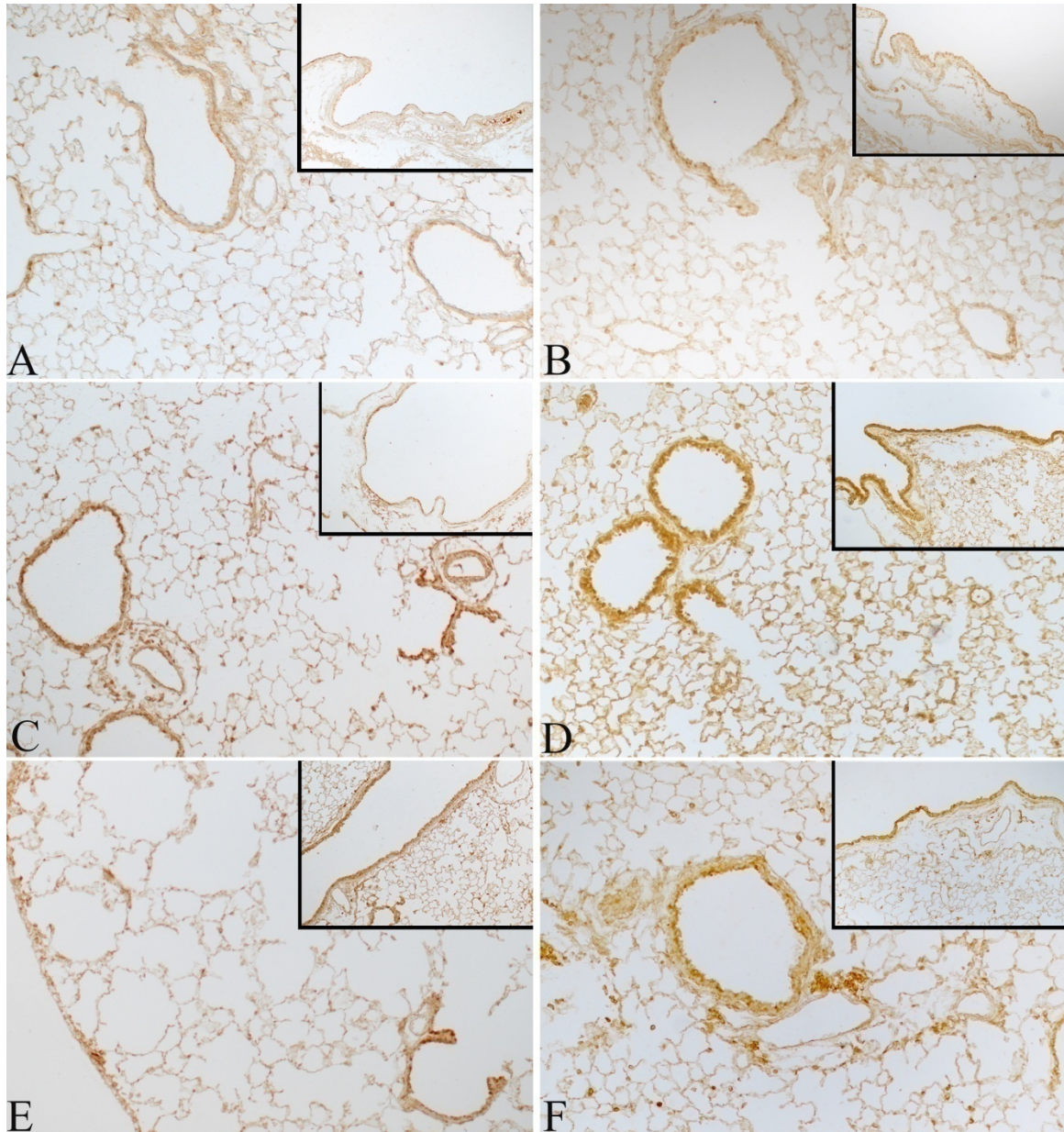
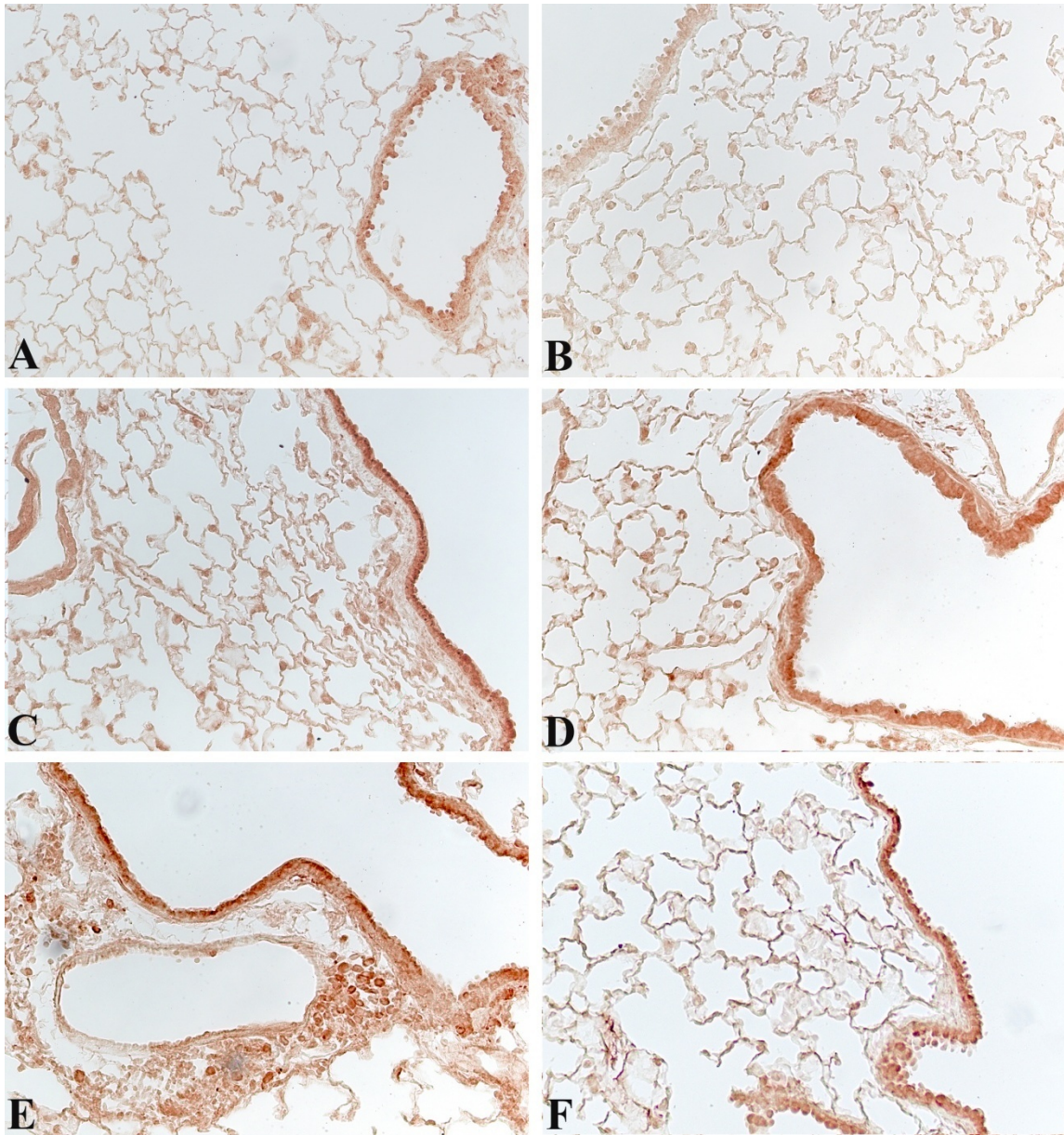


Figure 24. Immunohistochemical staining for P2X<sub>4</sub> on representative mouse sections of pulmonary tissue. (A) and (B) C57 Bl/6J and DBA/2 sections from mice exposed to room air. In (C) and (D) C57 Bl/6J and DBA/2 mice exposed to cigarette smoke for 7 months, respectively, are shown. (E) and (F) C57 Bl/6J and DBA/2 are from mice exposed to cigarette smoke for 11 months. Original magnification x100.

Purinergic signaling has been also suggested to be implicated in the pathogenesis of remodeling through the induction of different pro-fibrotic stimuli. Among them, we investigated the expression of **IL-6** in our mice. In Figure 25, we show the expression of this cytokine in C57 Bl/6J (C) and DBA/2 (D) mice exposed to cigarette smoke for 7 and 11 months (E and F). IL-6 is absent in air-control C57 Bl/6J (A) and DBA/2 (B) mice, increase progressively on bronchial epithelial cells between 7 (C) and 11 (E) months exposure in C57 Bl/6J. Differently, DBA/2 mice show only a faint stain at 7 months (D) and an increased expression at 11 months (F) of exposure.

Purinergic receptors, expressed in inflammatory cells like macrophages, promote and increase the expression of **Matrix Metalloproteinase-9 (MMP-9)**. The immunohistochemical reaction of MMP-9 on pulmonary tissue from smoking C57 Bl/6J (Fig. 26D) and DBA/2 mice (Fig. 26B) confirmed the increased expression of the enzyme when compared to air-control animals of the same strain (Fig. 26A and C).



*Figure 25. Immunohistochemical reaction for IL-6. Representative sections of mouse lungs from room air exposed (A) and cigarette smoke exposed C57Bl/6J mouse for 7(C) and 11 months (E). Representative lung sections from a control DBA/2 (B) and cigarette smoke exposed mouse at 7 (D) and 11 months (F). (A-F) original magnification x200.*

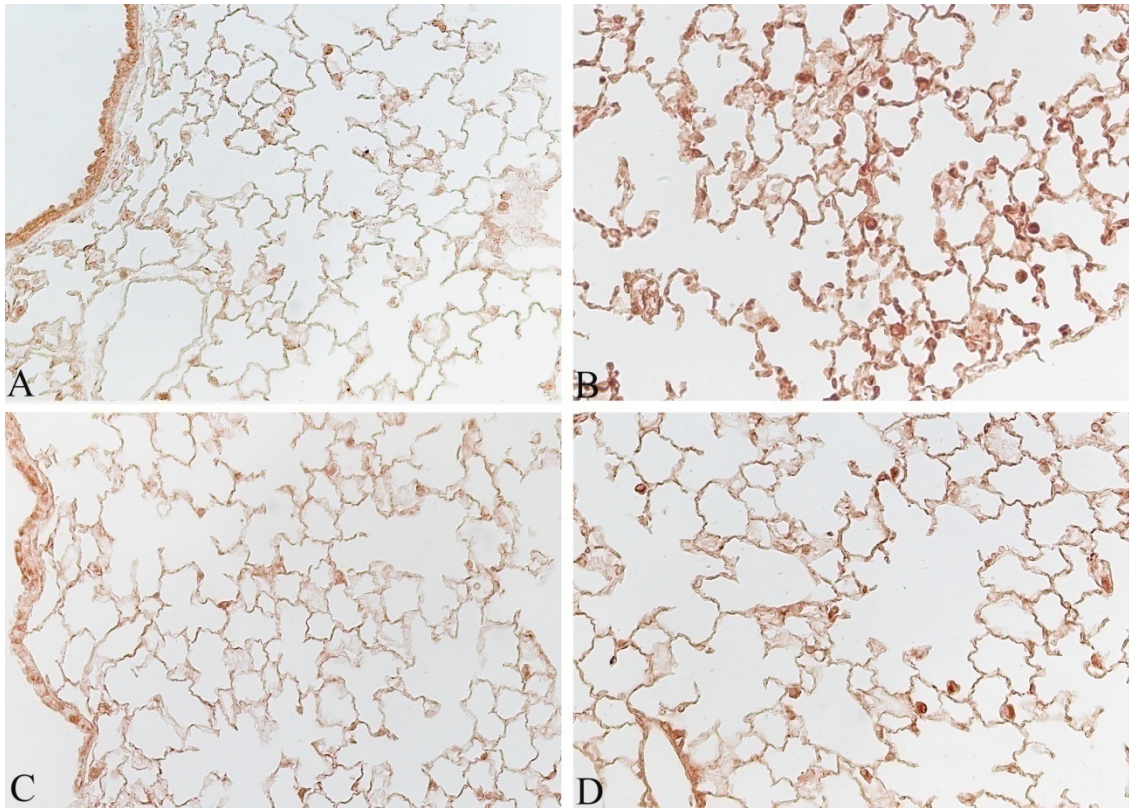


*Figure 26. Immunohistochemical reaction for MMP-9. Representative sections of lung tissue from room air-exposed (A) and a cigarette smoke exposed (B) DBA/2 mouse. Representative lung sections from a control (C) and a cigarette smoke exposed (D) C57Bl/J mouse. (A-D) Original magnification x200.*

	<b>C57 Bl/6J</b>	<b>DBA/2</b>
<b>Masson's trichrome stain</b>	After 7 months exposure C57 Bl/6J mice show only a small amount of collagen around bronchioles accompanied by a massive infiltration of inflammatory cells which increase during the following 4 months of treatment.	DBA/2 mice show, after the chronic exposure to cigarette smoke a marked peri-bronchiolar fibrosis with a progressive deposition of collagen after 7 and 11 months. A more consistent deposition of collagen can be seen at all time points when compared with C57 mice.
<b><math>\alpha</math>-SMA</b>	C57 mice exposed to cigarette smoke for 7 and 11 months show thick layers of <b><math>\alpha</math>-SMA</b> positive cells which progressively increase with time and circled main and distal bronchi as well as small vessels.	DBA/2 mice show the same pattern of expression and a more evident intensity of stain from 7 months onward when compared to C57 mice.
<b>PAS stain</b>	In C57 Bl/6J mice we can see a clear difference between control and smoking mice. After 7 and 11 months of exposure 75% and 70% of mice develop GCM respectively both in large and small airways with no significant difference between the two time points.	DBA/2 mice show, instead, only a few goblet cells localized mainly in large bronchi after 7 months of cigarette smoke exposure. A more consistent CGM can be appreciated after 11 months of exposure both in large and small airways but only 35% of animals of this strain develop GCM.
<b>TGF-<math>\beta</math></b>	Increased level of <b>TGF-<math>\beta</math></b> is appreciated in main and small bronchi at all time points.	Increased level of <b>TGF-<math>\beta</math></b> is appreciated in main and small bronchi at all time points.
<b>CTGF</b>	A progressive increase in stain positivity is seen in mice at 7 months of exposure, when the expression is localized mostly in bronchiolar epithelium, and 11 months of exposure when the expression is appreciable also in the muscular layer that circle bronchioles and vessels.	There is no appreciable difference in CTGF expression around parenchymal bronchioles at 7 and 11 months of smoke exposure. An increased expression is seen in the muscular layer of large airways and in small vessels after 11 months exposure.
<b>PDGF-B</b>	Expression is increased in intraparenchymal airways of C57 Bl/6J after 7 months exposure to CS. After 11 months a significant decrease is seen in small bronchi but remain expressed in airways and vessel SMC and inflammatory cells.	DBA/2 mice show a comparable expression in large and small airways at 7 and 11 months of exposure.
<b>8-OHdG</b>	After 4 months of CS exposure, a slight increase in positivity for 8-OHdG is appreciated on nuclei of parenchymal and bronchiolar cells, fibroblasts, myofibroblasts and SMC.	The proportion of staining nuclei of parenchymal and bronchiolar cells, fibroblasts, myofibroblasts and SMC is more consistent in DBA/2 than in C57 Bl/6J smoking mice after exposure to cigarette smoke for 4 months.
<b>CLEAVED</b>	In C57 Bl/6J control mice only a	DBA/2 control mice show no



<b>CASPASE 3</b>	<p>few positive stained cells in patchy areas are seen in bronchial and bronchiolar epithelial cells and sub-epithelial layer. After 7 months of CS exposure a massive increase in cell positivity in lung parenchyma and an almost absent positivity in sub-bronchiolar fibro-muscular layer is seen.</p> <p>At 11 months of exposure cleaved caspase-3 is almost absent around bronchi and it's decreased in lung parenchyma.</p>	<p>positive cells but a widespread positivity for Caspase-3 is detected in lung parenchyma after 7 months of CS exposure. Of interest DBA/2 mice show an increased expression of Cleaved Caspase-3 in epithelial bronchial cells when compared to control animal.</p>
<b>p16<sup>ink4A</sup></b>	<p>NO positivity can be seen in 1 months old C57 control mice and only few positive cells in 11 months old mice. After the exposure to CS for 4 months we see an increased positivity for p16 in bronchial epithelial cells, fibroblasts and myofibroblasts in sub-epithelial layer and AT-II.</p>	<p>Similar p16<sup>ink4A</sup> staining pattern can be seen in lung parenchyma of DBA/2 mice after 4 months of smoke exposure while a more marked staining is found in bronchiolar epithelial cells when compared to C57 Bl/6J mice.</p>
<b>PCNA</b>	<p>After 4 months of CS exposure mice of this strains show an increased number of bronchial cells nuclei positive for PCNA</p>	<p>In DBA/2 mice exposed to CS for 4 months the greatest increase in positive cells is localized in the sub-bronchiolar fibro-muscular layer and in subpleural areas.</p>
<b>MyoD</b>	<p>In control animal no MyoD expression can be seen in bronchioles an subpleural areas of C57 Bl/6J. Only a few positive cells can be appreciated in subpleural areas of C57 mice after 4 months cigarette smoke exposure.</p>	<p>An appreciable increase in MyoD expression is detectable in DBA/2 mice exposed to CS for 4 months in sub-bronchiolar fibro-muscular layer as well as in subpleural areas whereas no expression can be seen in control animals.</p>
<b>P2Y<sub>2</sub></b>	<p>P2Y<sub>2</sub> expression is slightly increased in C57 mice exposed to CS for 7 and 11 months mostly on large and small airways epithelial cells and in lung parenchyma with no appreciable difference between the two time points.</p>	<p>DBA/2 mice show, instead, a strong increase in positivity in lung tissue from mice exposed to CS for 7 months. After 11 months of CS exposure there is a decrease in the number of positive cells.</p>
<b>P2X<sub>4</sub></b>	<p>P2X<sub>4</sub> is constitutively expressed at low levels in control animals of both strains. C57 mice show an up-regulation of the receptor that is comparable at 7 and 11 months of exposure.</p>	<p>DBA/2 mice show a positive reaction especially in large airways after 7 months of exposure while the up-regulation of P2X<sub>4</sub> in bronchioles is seen after 11 months from the beginning of exposure.</p>
<b>IL-6</b>	<p>IL-6 is absent in air control C57 Bl/6J. Its expression increase progressively on bronchial epithelial cells between 7 and 11 months exposure in C57 Bl/6J.</p>	<p>Differently DBA/2 mice show no positive stain in control mice, only a faint stain at 7 months and an increased expression after 11 months of exposure.</p>

<b>MMP-9</b>	Expression is increased in pulmonary tissue from C57 Bl/6J exposed to cigarette smoke.	An increased expression of MMP-9 is appreciable in pulmonary tissue from DBA/2 mice exposed to cigarette smoke.
--------------	--	---

*Tab.4 Summary of the results obtained in the two mouse strains used in this study*

## DISCUSSION:

By a clinical point of view, chronic obstructive pulmonary disease (COPD) may be present in patients as one of several different phenotypes with different prognosis [Rennard SI *et al*, 2015 - Duffy S *et al*, 2015].

Although a lot of scientific studies has been carried out in the last twenty years, many facets of the pathogenesis of COPD are not fully understood.

Animal models of COPD involving cigarette smoking resulted of central importance to clarify the role of individual responses to develop the disease [Rahman I *et al*, 2017 - De Cunto G *et al*, 2020 (1)]. In particular, some mouse strains (such as C57 Bl/6J and DBA/2) develop significant emphysema when exposed to cigarette smoke for 7 months, while other mice (such as ICR) do not [Cavarra E *et al*, 2001]. Chronic cigarette smoke exposure leads to various phenotypes of disease in the different mouse strains [Bartalesi B *et al*, 2005 - Lucattelli M *et al*, 2005 - De Cunto G *et al*, 2011 - De Cunto G *et al*, 2020 (2) - Lunghi B *et al*, 2015], which can also be found in human patients.

Very recent studies conducted in both humans and animals indicate that innate inflammatory cells activated by different stimuli on cell surface are needed to develop pulmonary changes caused by cigarette smoking [De Cunto G *et al*, 2016 - Cardini S *et al*, 2012 - Cicko S *et al*, 2010 - Lucattelli M *et al*, 2011 - Lommatzsch M *et al*, 2010 - Fineschi S *et al*, 2013 - Stogsdill MP *et al*, 2013 - Robinson AB *et al*, 2012 - Lazar Z *et al*, 2016 - Atzori L *et al*, 2009]. Smoking exposure induces pro-inflammatory response through the activation of pattern recognition receptors (PRRs) by damage-associated molecular patterns (DAMPs) release (i.e. AGE, endogenous ATP, formyl peptides, HMGB1, MyD88 etc.) [Cardini S *et al*, 2012 - Cicko S *et al*, 2010 - Lucattelli M *et al*,

2011 - Lommatzsch M *et al*, 2010 - Fineschi S *et al*, 2013 - Lazar Z *et al*, 2016 - Waseda K *et al*, 2015 - Stockley RA *et al*, 1994 - De Cunto G *et al*, 2018].

Studies carried out in animals and man suggest that alveolar macrophages and neutrophils play a central role in pathophysiology of COPD and may orchestrate the chronic inflammatory responses [Barnes PJ, 2014]. In particular, as reported in recent studies from our and other labs [De Cunto G *et al*, 2020 (3)], the natural plasticity of macrophages give rise to different cell populations with different phenotype and functions, capable of influencing the inflammatory responses, and therefore destruction, repair and remodeling of pulmonary structures.

These changes that may be present at different extent may underpin the different clinical phenotype of the disease.

As reported above, some murine strains mirror some human phenotypes after smoke exposure. It was of interest to investigate in these strains whether changes in different endogenous factors, whose expression can influence alveolar destruction, repair and anatomical remodeling, are associated with changes characterizing different phenotypes of the disease. This study has been approached by using immunohistochemistry in order to have information on the expression and distribution these factors in pulmonary structures at selected time points after the starting of smoke exposure.

For this purpose, we chose C57 Bl/6J, which show significant emphysema associated with goblet cell metaplasia in airways epithelium after chronic cigarette smoke exposure, and DBA/2 mice that develop changes similar to those described in "pulmonary fibrosis/emphysema syndrome" in humans [Cottin V *et al*, 2005].

My work has been carried out in these strains in order to complete and verify by immunohistochemistry the expression of factors whose gene profile changes were previously observed by microarray [Cavarra E *et al*, 2009] and real-time PCR analyses [De Cunto G *et al*, 2018]. Therefore, this study was conducted on gene products, (such as enzymes, cytokines, surface receptors and transcription factors), which are able to modulate cell phenotypic changes and may induce senescence, apoptosis and proliferation of cells involved in repair and remodeling processes that characterize the models mentioned above.

It is well recognized that **apoptosis** plays important role in cell renewal in pulmonary tissue. This process has been investigated by evaluating the presence in pulmonary cells of **cleaved caspase-3** by immunostaining. No difference in terms of distribution and intensity of cleaved (activated) caspase-3 has been observed in lung parenchyma, in peri-bronchiolar and peri-bronchial areas between the C57 Bl/6J and DBA/2 mice after 7 months of cigarette smoke exposure. On the contrary, some differences in distribution of cleaved caspase-3 positive cells are seen between the two mouse strains in the epithelial layers of airways. Our findings suggest that a specific variation in apoptosis rate does not contribute, at least in peri-bronchial and peri-bronchiolar areas, to the differences in the accumulation of mesenchymal cells and in the fibrotic remodeling we observe beneath the airways epithelial layers in the two strains of mice. Slight differences are observed between the two strains of smoking mice in the expression of fibrogenic cytokines at the various time points after cigarette smoke exposure. However, even these differences by alone fail to explain the obvious differences we found in fibrous remodeling of the peri-bronchial and peri-bronchial areas of the two mouse strains. A marked deposition of collagen (stained in light green) and a major number of  $\alpha$ -SMA positive cells that progressively increase with time is

clearly perceivable in DBA/2 mouse. This may be also appreciated in several subpleurical areas of DBA/2 mouse.

Of interest, the transcription factor **MyoD**, is expressed in major extent in peri-bronchial and peri-bronchiolar cells of smoking DBA/2 mice. It has been recently reported that MyoD may impair myofibroblast dedifferentiation and alters the apoptotic clearance of senescent cells contributing to non resolving fibrosis [Kato K *et al*, 2020]. Therefore, an hyperexpression of MyoD in DBA/2 mice may accelerate the fibrotic remodeling. The impaired apoptotic clearance of senescent fibroblasts and myofibroblasts present in subepithelial layers (as revealed after immunohistochemical staining for **p16<sup>ink4A</sup>**) together with the continuous proliferative (**PCNA**) and metabolic stimuli by **fibrotic cytokines** (such as TGF- $\beta$ , PDGF-B and CTGF) may offer an explanation for the differences in terms of fibrotic remodeling we observe between the two strains of mice at the different time points. Evidence for such a view is supported by the immunohistochemical findings we observe in the subepithelial cell layers after PCNA staining. A major number of **PCNA** positive cells, which undergo to division, can be appreciated in DBA/2 mice in respect to C57 Bl/6J strain. However, we cannot rule out that the difference we see could be due a major sensitivity of DBA/2 cells to proliferate under the stimulation of fibrotic cytokines.

Inflammation is a driving mechanism in the development and progression of COPD. Neutrophils and macrophages are essential components of inflammation that in concert to other cells of innate immunity (such as eosinophils, mast cells, dendritic cells, NK cells), cells of the adaptive immunity (B and T lymphocytes) and structural cells of the lung (i.e. fibroblasts, endothelial, airway and alveolar epithelial cells) release a lot of inflammatory mediators (enzymes, oxidants and chemokines) that may cause destructive changes to lung

parenchyma and/or remodeling and narrowing processes of small airways [Rangasamy T *et al*, 2006].

During the early stages of the disease, both neutrophils and macrophages, recruited by the action of cigarette smoke, play an essential role in the destructive processes of the lung parenchyma and alveolar attachments of the small airways by releasing enzymes (such as elastase, MMP-9, etc) or oxygen reactive species. These compounds cause necrosis of epithelial cells, which release “alarmins” (DAMPs) which activate pathways through activation of surface receptors that amplify the inflammatory. Alarmins include formyl peptides, advanced glycation by products, ATP and UTP, and other products derived from necrotic cells. In particular, ATP and UTP are the major ligands of **purinergic receptors P2X<sub>4</sub>, P2X<sub>7</sub> and P2Y<sub>2</sub>**, which are involved in COPD pathogenesis. On the basis of the findings we report, we can conclude that the activation of purinergic receptors may be ascribed to the massive necrosis of alveolar epithelial cells caused by enzyme release (such as **MMP-9**) and oxidative damage (as revealed by **8-OHdG**), which characterize, a different extent, C57 Bl/6J and DBA/2 lung responses.

Both strains of mice show in airway epithelium the presence of numerous goblet cells (**PAS** positive cells), which are part of a metaplastic process in mice. Goblet cell metaplasia develops in C57 Bl/6J mice earlier in time (at 4 months after cigarette smoke exposure) in respect to DBA/2 mice, in which it appears only in some animals (35%) at 11 months. This observation confirms what reported in previous paper from our lab [Bartalesi B *et al*, 2005]. The more apparent rate of apoptosis we observe in airway epithelial cells of DBA/2 mice may play a role in late appearance of goblet cell metaplasia in this strain.

## CONCLUSIONS:

In conclusions, this study carried out in smoking mice from C57 BL/6J and DBA/2 mouse strains suggests that individual responses in terms endogenous factors influence alveolar destruction, repair and anatomical remodeling after chronic exposure to cigarette smoke. The difference in the distribution of changes in pulmonary structures can lead to dysfunctional responses [De Cunto G *et al*, 2020 (2)], which in some respects are similar to those that may characterize COPD phenotypes in humans.

However, much more work in mouse models is necessary to gain insight into the underlying mechanisms of the disease and to search and develop new compounds with a potential therapeutic activity for COPD patients.

Mouse models of COPD involving cigarette smoke should be essential components of this program and the findings reported here could offer some help, albeit modest, to such research.



## REFERENCES:

Abbracchio MP and Burnstock G, 1998. "*Purinergic Signaling: Patophysiological roles*" Jpn J Pharmacol 78, 113-145

Abdollahi A, Li M, Ping G, Plathow C, Domhan S, Kiessling F, Lee LB, McMahon G, Grone HJ, Lipson KE and Huber PE, 2005. "*Inhibition of platelet derived growth factor signaling attenuates pulmonary fibrosis*" J Exp Med 201, 925-935

Aliagas E, Muñoz-Esquerre M, Cuevas E, Careta O, Huertas D, López-Sánchez M, Escobar I, Dorca J and Santos S, 2018. "*Is the purinergic pathway involved in the pathology of COPD? Decreased lung CD39 expression at initial stages of COPD*" Respir Res 19, 103

Antoniades HN, Bravo MA, Avila RE, Galanopoulos T, Neville-Golden J, Maxwell M and Selman M, 1990. "*Platelet-derived growth factor in idiopathic pulmonary fibrosis*" J Clin Invest 86, 1055-1064

Atzori L, Lucattelli M, Scotton CJ, Laurent GJ, Bartalesi B, De Cunto G, Lunghi B, Chambers RC and Lungarella G, 2009. "*Absence of proteinase-activated receptor-1 signaling in mice confers protection from fMLP-induced goblet cell metaplasia*" Am J Respir Cell Mol Biol 41, 680-687

Barnes PJ, 2014. "*Cellular and molecular mechanisms of chronic obstructive pulmonary disease*" Clin Chest Med 35, 71-86

Bartalesi B, Cavarra E, Fineschi S, Lucattelli M, Lunghi B, Martorana PA and Lungarella G, 2005. "*Different lung responses to cigarette smoke in two strains of mice sensitive to oxidants*" Eur Respir J 25, 15-22

- Bonner JC, 2004. "*Regulation of PDGF and its receptors in fibrotic diseases*" Cytokine Growth Factor Rev 15, 255-273
- Bonnaud P, Martin G, Margetts PJ, Ask K, Robertson J, Gauldie j and Kolb M, 2004. "*Connective tissue growth factor is crucial to inducing a profibrotic environment in "fibrosis-resistant" BALB/c mouse lungs*" Am J Respir Cell Mol Biol 31, 510-516
- Boue-Grabot E, Archambault V and Seguela P, 2000. "*A protein kinase C site highly conserved in P2X subunits controls the desensitization kinetics of P2X2 ATP-gated channels*" J Biol Chem 275, 10190-10195
- Burnstock G, 2007. "*Purine e Pyrimidine receptors*" Cell Mol Life Sci 64, 1471-1483
- Burnstock G, Brouns I, Adriaensen D and Timmermans JP, 2012. "*Purinergic signaling in the airways*" Pharmacol Rev 64, 834-868
- Cardini S, Dalli J, Fineschi S, Perretti M, Lungarella G and Lucattelli M, 2012. "*Genetic ablation of the fpr1 gene confers protection from smoking-induced lung emphysema in mice*" Am J Respir Cell Mol Biol 47, 332-339
- Cavarra E, Bartalesi B, Lucattelli M, Fineschi S, Lunghi B, Gambelli F, Ortiz LA, Martorana PA and Lungarella G, 2001. "*Effects of cigarette smoke in mice with different levels of  $\alpha$ 1-proteinase inhibitor and sensitivity to oxidants*" Am J Respir Crit Care Med 164, 886-890
- Cavarra E, Fardin P, Fineschi S, Ricciardi A, De Cunto G, Sallustio F, Zorzetto M, Luisetti M, Pfeffer U, Lungarella G and Varesio L, 2009. "*Early response of gene clusters is associated with mouse lung resistance or sensitivity to cigarette smoke*" Am J Physiol Lung Cell Mol Physiol 296, L418-429

Chambers JK, Macdonald LE, Sarau HM, Ames RS, Freeman K, Foley JJ, Zhu Y, McLaughlin MM, Murdock P, McMillan L, Trill J, Swift A, Aiyar N, Taylor P, Vawter L, Naheed S, Szekeres P, Hervieu G, Scott C, Watson JM, Murphy AJ, Duzic E, Klein C, Bergsma DJ, Wilson S and Livi GP, 2000. "*A G protein-coupled receptor for UDP-glucose*" J Biol Chem 275, 10767-10771

Chen H, Xia Q, Feng X, Cao F, Yu H, Song Y and Ni X, 2016. "*Effect of P2X4R on airway inflammation and airway remodeling in allergic airway challenge in mice*" Mol Med Rep 13, 697-704

Chiappara G, Gjomarkaj M, Sciarrino S, Vitulo P, Pipitone L and Pace E, 2014. "*Altered expression of p21, activated caspase-3, and PCNA in bronchiolar epithelium of smokers with and without chronic obstructive pulmonary disease*" Exp Lung Res 40, 343-353

Chung KF and Adcock IM, 2008. "*Multifaceted mechanisms in COPD: inflammation, immunity, and tissue repair and destruction*" Eur Respir J 31, 1334-1356

Churg A, Tai H, Coulthard T, Wang R and Wright JL, 2006. "*Cigarette Smoke Drives Small Airway Remodeling by Induction of Growth Factors in the Airway Wall*" Am J Respir Crit Care Med 174, 1327-1334

Churg A and Wright JL, 2009. "*Testing drugs in animal Models of Cigarette Smoke-Induced Chronic Obstructive Pulmonary Disease*" Proc Am Thorac Soc 6, 550-556

Cicko S, Lucattelli M, Müller T, Lommatzsch M, De Cunto G, Cardini S, Sundas W, Grimm M, Zeiser R, Dürk T, Zissel G, Boeynaems JM, Sorichter S, Ferrari D, Di Virgilio F, Virchow JC, Lungarella G and Idzko M, 2010. "*Purinergic receptor inhibition prevents the development of smoke-induced lung injury and emphysema*" J Immunol 185, 688-97

Cosio MG, Hale KA and Niewoehner DE, 1980. "*Morphologic and Morphometric Effects of prolonged Cigarette Smoking on the Small Airways*" Am Rev Resp Dis 122, 265-271

Cottin V, Nunes H, Brillet PY, Delaval P, Devouassoux G, Tillie-Leblond I, Israel-Biet D, Court-Fortune I, Valeyre D, Cordier JF and Groupe d'Etude et de Recherche sur les Maladies Orphelines Pulmonaires, 2005. "*Combined pulmonary fibrosis and emphysema: a distinct underrecognised entity*" Eur Respir J 26, 586-593

Curtis JL, Freeman CM and Hogg JC, 2007. "*The Immunopathogenesis of Chronic Obstructive Pulmonary Disease*" Proc Am thorac Soc 4, 512-521

De Cunto G, Cardini S, Cirino G, Geppetti P, Lungarella G and Lucattelli M, 2011. "*Pulmonary hypertension in smoking mice over-expressing protease-activated receptor-2*" Eur Respir J 37, 823-834

De Cunto G, Lunghi B, Bartalesi B, Cavarra E, Fineschi S, Olivieri C, Lungarella G and Lucattelli M, 2016. "*Severe Reduction in Number and Function of Peripheral T Cells Does Not Afford Protection toward Emphysema and Bronchial Remodeling Induced in Mice by Cigarette Smoke*" Am J Pathol 186, 1814-1824

De Cunto G, Bartalesi B, Cavarra E, Balzano E, Lungarella G and Lucattelli M, 2018. "*Ongoing Lung Inflammation and Disease Progression in Mice after Smoking Cessation: Beneficial Effects of Formyl-Peptide Receptor Blockade*" Am J Pathol 188, 2195-2206

De Cunto G, Cavarra E, Bartalesi B, Lucattelli M and Lungarella G, 2020 (1). "*Innate Immunity and Cell Surface Receptors in the Pathogenesis of COPD: Insights from Mouse Smoking Models*" Int J Chron Obstruct Pulmon Dis 15, 1143-1154

De Cunto G, Brancaleone V, Riemma MA, Cerqua I, Vellecco V, Spaziano G, Cavarra E, Bartalesi B, D'Agostino B, Lungarella G, Cirino G, Lucattelli M and Roviezzo F, 2020 (2).

"Functional contribution of sphingosine-1-phosphate to airway pathology in cigarette smoke-exposed mice" *Br J Pharmacol* 177, 267-281

De Cunto G, Cavarra E, Bartalesi B, Lungarella G and Lucattelli M, 2020 (3). "Alveolar Macrophage Phenotype and Compartmentalization Drive Different Pulmonary Changes in Mouse Strains Exposed to Cigarette Smoke" *COPD* 17, 429-443.

Deslee G, Woods JC, Moore C, Conradi SH, Gierada DS, Atkinson JJ, Battaile JT, Liu L, Patterson GA, Adair-Kirk TL, Holtzman MJ and Pierce RA, 2009. "Oxidative damage to nucleic acids in severe emphysema" *Chest* 135, 965-974

Duffy S, Weir M and Criner GJ, 2015. "The complex challenge of chronic obstructive pulmonary disease" *Lancet Respir Med* 3, 917-919

Eltom S, Stevenson CS, Rastrick J, Dale N, Raemdonck K, Wong S, Catley MC, Belvisi MG and Birrell MA, 2011. "P2X7 receptor and caspase 1 activation are central to airway inflammation observed after exposure to tobacco smoke" *PLoS One* 6, e24097

Ennion S, Hagan S and Evans RJ, 2000. "The role of positively charged amino acids in ATP recognition by human P2X1 receptors" *J Biol Chem* 275, 29361-29367

Erb L, Garrad R, Wang Y, Quinn T, Turner JT and Weisman GA, 1995. "Site-directed mutagenesis of P2U purinoceptors. Positively charged amino acids in transmembrane helices 6 and 7 affect agonist potency and specificity" *J Biol Chem* 270, 4185-4188

Fineschi S, De Cunto G, Facchinetti F, Civelli M, Imbimbo BP, Carnini C, Villetti G, Lunghi B, Stochino S, Gibbons DL, Hayday A, Lungarella G and Cavarra E, 2013. "Receptor for advanced glycation end products contributes to postnatal pulmonary development and adult lung maintenance program in mice" *Am J Respir Cell Mol Biol* 48, 164-171

- Fischer W and Krügel U, 2007. *"P2Y Receptors: Focus on Structural, Pharmacological and Functional Aspects in the Brain"* Curr med chem 14, 2429-2455
- Harden TK, Sesma JI, Fricks IP and Lazarowski ER, 2010. *"Signalling and pharmacological properties of the P2Y receptor"* Acta Physiol 199, 149-160
- Hecker L, Jagirdar R, Jin T and Thannickal VJ, 2011. *"Reversible differentiation of myofibroblasts by MyoD"* Exp Cell Res 317, 1914-1921
- Hinz B, Phan SH, Thannickal VJ, Prunotto M, Desmoulière A, Varga J, De Wever G, Mareel M and Gabbiani G, 2012. *"Recent developments in myofibroblast biology: paradigms for connective tissue remodeling"* Am J Pathol 180, 1340-1355
- Hogg JC, 2004. *"Pathophysiology of airflow limitation in chronic obstructive pulmonary disease"* Lancet 364, 709-721
- Humbert M, Morrell NW, Archer SL, Stenmark KR, MacLean MR, Lang IM, Christman BW, Weir EK, Eickelberg O, Voelkel NF and Rabinovitch M, 2004. *"Cellular and molecular pathobiology of pulmonary arterial hypertension"* J Am Coll Cardiol 43, 13S-24S
- Idzko M, Ferrari F and Eltzschig HK, 2014. *"Nucleotide signaling during inflammation"* Nature 509, 310-317
- Ingram JL, Rice AB, Geisenhoffer K, Madtes DK and Bonner JC, 2004. *"IL-13 and IL-1 promote lung fibroblast growth through coordinated upregulation of PDGF-AA and PDGF-R"* FASEB J 18, 1132-1134
- Jeffery PK, 1999. *"Differences and similarities between chronic obstructive pulmonary disease and asthma"* Clin Exp Allergy 29, 14-26

Kato K, Logsdon NJ, Shin YJ, Palumbo S, Knox A, Irish JD, Rounseville SP, Rummel SR, Mohamed M, Ahmad K, Trinh JM, Kurundkar D, Knox KS, Thannickal VJ and Hecker L, 2020. "*Impaired Myofibroblast Dedifferentiation Contributes to Non resolving Fibrosis in Aging*" Am J Respir Cell Mol Biol 62, 633-644

Kim V, Rogers TJ and Criner GJ, 2008. "*New Concepts in the Pathobiology of Chronic Obstructive Pulmonary Disease*" Proc Am Thorac Soc 5, 478-485

Kovacs EJ and DiPietro LA, 1994. "*Fibrogenic cytokines and connective tissue production*" FASEB J 8, 854-861

Lasky JA, Ortiz LA, Tonthat B, Hoyle GW, Corti M, Athas G, Lungarella G, Brody A and Friedman M, 1998. "*Connective tissue growth factor mRNA expression is upregulated in bleomycin-induced lung fibrosis*" Am J Physiol 275, L365-L371

Lazar Z, Müllner N, Lucattelli M, Ayata CK, Cicko S, Yegutkin GG, De Cunto G, Müller T, Meyer A, Hossfeld M, Sorichter S, Horvath I, Virchow CJ, Robson SC, Lungarella G and Idzko M, 2016. "*NTPDase1/CD39 and aberrant purinergic signalling in the pathogenesis of COPD*" Eur Respir J 47, 254-263

Li B and Wang JHC, 2011. "*Fibroblasts and myofibroblasts in wound healing: Force generation and measurement*" J Tissue Viability 20, 108-120

Liang GB and He ZH, 2019. "*Animal models of emphysema*" Chin Med J (Engl) 132, 2465-2475

Lommatzsch M, Cicko S, Müller T, Lucattelli M, Bratke K, Stoll P, Grimm M, Dürk T, Zissel G, Ferrari D, Di Virgilio F, Sorichter S, Lungarella G, Virchow JC and Idzko M, 2010. "*Extracellular Adenosine Triphosphate and Chronic Obstructive Pulmonary Disease*" Am J Respir Crit Care Med 18, 928-934

- Lucattelli M, Bartalesi B, Cavarra E, Fineschi S, Lunghi B, Martorana PA and Lungarella G, 2005. "*Is neutrophil elastase the missing link between emphysema and fibrosis? Evidence from two mouse models*" *Respir Res* 6, e83
- Lucattelli M, Cicko S, Müller T, Lommatzsch M, De Cunto G, Cardini S, Sundas W, Grimm M, Zeiser R, Dürk T, Zissel G, Sorichter S, Ferrari D, Di Virgilio F, Virchow JC, Lungarella G and Idzko M, 2011. "*P2X7 receptor signaling in the pathogenesis of smoke-induced lung inflammation and emphysema*" *Am J Respir Cell Mol Biol* 44, 423-429
- Lungarella G, Fonzi L and Ermini G, 1983. "*Abnormalities of bronchial cilia in patients with chronic bronchitis. An ultrastructural and quantitative analysis*" *Lung* 161, 147-156
- Lunghi B, De Cunto G, Cavarra E, Fineschi S, Bartalesi B, Lungarella G and Lucattelli M, 2015. "*Smoking p66Shc knocked out mice develop respiratory bronchiolitis with fibrosis but not emphysema*" *PLoS One* 10, e0119797
- McNee W, 1994 (1). "*Pathophysiology of Cor Pulmonale in Chronic Obstructive Pulmonary Disease. Part Two*" *Am J Respir Crit Care Med* 150, 1158-1168
- McNee W, 1994 (2). "*Pathophysiology of Cor Pulmonale in Chronic Obstructive Pulmonary Disease. Part One*" *Am J Respir Crit Care Med* 150, 883-852
- Mortaz E, Braber S, Nazary M, Givi ME, Nijkamp FP and Folkerts G, 2009. "*ATP in the pathogenesis of lung emphysema*" *Eur J Pharmacol* 619, 92-96
- Müller T, Fay S, Vieira RP, Karmouty-Quintana H, Cicko S, Ayata K, Zissel G, Goldmann T, Lungarella G, Ferrari D, Di Virgilio F, Robaye B, Boeynaems JM, Blackburn MR and Idzko M, 2017. "*The purinergic receptor subtype P2Y<sub>2</sub> mediates chemotaxis of neutrophils and fibroblasts in fibrotic lung disease*" *Oncotarget* 8, 35962-35972.



Newbolt A, Stoop R, Virginio C, Surprenant A, North RA, Buell G and Rassendren F, 1998. "*Membrane topology of an ATP-gated ion channel (P2X receptor)*" J Biol Chem 273, 15177-15182

North RA, 2002. "*Molecular Physiology of P2X receptors*" Physiol Rev 82, 1013-1067

Pauwels RA, Buist AS, Calverley PMA, Jenkins CR and Hurd SS, 2001. "*Global Strategy for the Diagnosis, Management and Prevention of Chronic Obstructive Pulmonary Disease. NHLBI/WHO Global Initiative for Chronic Obstructive Lung Disease (GOLD)*" Am J Respir Crit Care Med 163, 1256-1276

Perros F, Montani D, Dorfmüller P, Durand-Gasselin I, Tcherakian C, Le Pavec J, Mazmanian M, Fadel E, Mussot S, Mercier O, Herve P, Emilie D, Eddahibi S, Simonneau G, Souza R and Humbert M, 2008. "*Platelet-derived growth factor expression and function in idiopathic pulmonary arterial hypertension*" Am J Respir Crit Care Med 178, 81-88

Phan SH, 2002. "*The Myofibroblast in Pulmonary Fibrosis*" CHEST J 122, 286S-289S

Pini L, Pinelli V, Modina D, Bezzi M, Tiberio L and Tantucci C, 2014. "*Central airway remodeling in COPD patients*" Int J Chron Obstruct Pulmon Dis 9, 927-933

Rahman I, De Cunto G, Sundar IK and Lungarella G, 2017. "*Vulnerability and Genetic Susceptibility to Cigarette Smoke-Induced Emphysema in Mice*" Am J Respir Cell Mol Biol 57, 270-271

Ralevic V and Burnstock G, 1998. "*Receptors for purines and pyrimidines*" Pharmacol 50, 415-475

Rangasamy T, Misra V, Lee H, Singh A and Biswal S, 2006. "*Differences in Nrf2 activity between emphysema resistant (ICR) and susceptible (C57Bl/6J) mice strains in response to acute cigarette smoke exposure*" Proc Am Thor Soc 3, A129

Rennard SI, Locantore N, Delafont B, Tal-Singer R, Silverman EK, Vestbo J, Miller BE, Bakke P, Celli B, Calverley PM, Coxson H, Crim C, Edwards LD, Lomas DA, MacNee W, Wouters EF, Yates JC, Coca I and Agustí A, 2015. "*Evaluation of COPD Longitudinally to Identify Predictive Surrogate Endpoints. Identification of five chronic obstructive pulmonary disease subgroups with different prognoses in the ECLIPSE cohort using cluster analysis*" Ann Am Thorac Soc 12, 303-312.

Riteau N, Gasse P, Fauconnier L, Gombault A, Couegnat M, Fick L, Kanellopoulos J, Quesniaux VF, Marchand-Adam S, Crestani B, Ryffel B and Couillin I, 2010. "*Extracellular ATP is a danger signal activating P2X7 receptor in lung inflammation and fibrosis*" Am J Respir Crit Care Med 182, 774-783

Robert S, Gicquel T, Victoni T, Valença S, Barreto E, Bailly-Maître B, Boichot E and Lagente V, 2016. "*Involvement of matrix metalloproteinases (MMPs) and inflammasome pathway in molecular mechanisms of fibrosis*" Biosci Rep 36, e00360

Robinson AB, Stogsdill JA, Lewis JB, Wood TT and Reynolds PR, 2012. "*RAGE and tobacco smoke: insights into modeling chronic obstructive pulmonary disease*" Front Physiol 3, 301

Saito A, Horie M and Nagase T, 2018. "*TGF- $\beta$  Signaling in Lung Health and disease*" Int J Mol Sci 19, 2460

Saito F, Tasaka S, Inoue K, Miyamoto K, Nakano Y, Ogawa Y, Yamada W, Shiraishi Y, Hasegawa N, Fujishima S, Takano H and Ishizaka A, 2008. "*Role of interleukin-6 in*

*bleomycin-induced lung inflammatory changes in mice*" Am J Respir Cell Mol Biol 38, 566-571

Saitoh M, 2015. "*Epithelial-mesenchymal transition is regulated at post-transcriptional levels by transforming growth factor- $\beta$  signaling during tumor progression*" Cancer Sci 106, 481-488

Senior RM and Anthonisen NR, 1998. "*Chronic Obstructive Pulmonary Disease (COPD)*" Am J Respir Crit Care Med 157, 139-147

Serrano AL and Muñoz-Cánoves P, 2010. "*Regulation and dysregulation of fibrosis in skeletal muscle*" Exp Cell Res 316, 3050-3058

Smith FM, Humphrey PPA and Murrel-Lagnado RD, 1999. "*Identification of amino acids within the P2X2 receptor C-terminus that regulate desensitization*" J Physiol 520, 91-99

Snider GL, 1989. "*Chronic obstructive pulmonary disease: risk factors, pathophysiology and pathogenesis*" Annu Rev Med 40, 411-429.

Stockley RA, Grant RA, Llewellyn-Jones CG, Hill SL and Burnett D, 1994. "*Neutrophil formyl-peptide receptors. Relationship to peptide-induced responses and emphysema*" Am J Respir Crit Care Med 149, 464-468

Stogsdill MP, Stogsdill JA, Bodine BG, Fredrickson AC, Sefcik TL, Wood TT, Kasteler SD and Reynolds PR, 2013. "*Conditional overexpression of receptors for advanced glycation end-products in the adult murine lung causes airspace enlargement and induces inflammation*" Am J Respir Cell Mol Biol 49, 128-34

Surprenant A, Rassendren FA, Kawashima E, North RA and Buell G, 1996. "*The cytolytic P2Z receptor for extracellular ATP identified as a P2X receptor (P2X<sub>7</sub>)*" *Science* 272, 735-738

Thurlbeck WM, 1967 (1). "*Internal surface area of non emphysematous lungs*" *Am Rev Respir Dis*, 95, 765-773

Thurlbeck WM, 1967 (2). "*Measurement of Pulmonary Emphysema*" *Am Rev Resp Dis* 95, 752-764

Torres GE, Egan TM and Voigot MM, 1998. "*N-Linked glycosylation is essential for the functional expression of the recombinant P2X<sub>2</sub> receptor*" *Biochemistry* 37, 4845-4851.

van der Vliet A and Bove PF, 2011. "*Purinergic signaling in wound healing and airway remodeling*" *Subcell Biochem* 55, 139-157

Vignola AM, Chanez P, Chiappara G, Merendino A, Pace E, Rizzo A, Rocca AM, Bellia V, Bonsignore G and Bousquet J, 1997. "*Transforming Growth Factor- $\beta$  Expression in Mucosal Biopsies in Asthma and Chronic Bronchitis*" *Am J Respir Crit Care Med* 156, 591-599

Virginio C, MacKenzie A, Rassendren FA, North RA and Surprenant A, 1999 (1). "*Pore dilation of neuronal P2X receptor channels*" *J Physiol* 2, 315-321

Virginio C, MacKenzie A, North RA and Surprenant A, 1999 (2) "*Kinetics of cell lysis, dye uptake and permeability changes in cells expressing the rat P2X<sub>7</sub> receptor*" *J Physiol* 519, 335-346

- Wang L, Feng X, Hu B, Xia Q, Ni X and Song Y, 2018. "*P2X4R promotes airway remodeling by acting on the phenotype switching of bronchial smooth muscle cells in rats*" Purinergic Signal 14, 433-442
- Waseda K, Miyahara N, Taniguchi A, Kurimoto E, Ikeda G, Koga H, Fujii U, Yamamoto Y, Gelfand EW, Yamamoto H, Tanimoto M and Kanehiro A, 2015. "*Emphysema requires the receptor for advanced glycation end-products triggering on structural cells*" Am J Respir Cell Mol Biol 52, 482-491
- Weinhold K, Krause-Buchholz U, Rödel G, Kasper M and Barth K, 2010. "*Interaction and interrelation of P2X7 and P2X4 receptor complexes in mouse lung epithelial cells*" Cell Mol Life Sci 67, 2631-2642
- Willis BC, duBois RM and Borok Z, 2006. "*Epithelial origin of myofibroblasts during fibrosis in the lung*" Proc Am Thorac Soc 3, 377-382
- Winkelmann VE, Thompson KE, Neuland K, Jaramillo AM, Fois G, Schmidt H, Wittekindt OH, Han W, Tuvim MJ, Dickey BF, Dietl P and Frick M, 2019. "*Inflammation-induced upregulation of P2X<sub>4</sub> expression augments mucin secretion in airway epithelia*" Am J Physiol Lung Cell Mol Physiol 316, L58-L70
- Wynn T, 2008. "*Cellular and Molecular Mechanism of Fibrosis*" J Pathol 214, 199-210
- Yamamoto K, Sokabe T, Matsumoto T, Yoshimura K, Shibata M, Ohura N, Fukuda T, Sato T, Sekine K, Kato S, Isshiki M, Fujita T, Kobayashi M, Kawamura K, Masuda H, Kamiya A and Ando J, 2006. "*Impaired flow-dependent control of vascular tone and remodeling in P2X<sub>4</sub>-deficient mice*" Nat Med 12, 133-137

Zech A, Wiesler B, Ayata CK, Schlaich T, Dürk T, Hoßfeld M, Ehrat N, Cicko S and Idzko M, 2016. "*P2rx4 deficiency in mice alleviates allergen-induced airway inflammation*" *Oncotarget* 7, 80288-80297